ÇUKUROVA UNIVERSITY
INSTITUTE OF NATURAL AND APPLIED SCIENCE

MSc THESIS

Makki AZZAMAN

SYNTHESIS OF COUMARIN-SCHIFF BASE DERIVATIVES AND INVESTIGATION PHOTOCHEMICAL PROPERTIES

DEPARTMENT OF CHEMISTRY

ADANA, 2022

ABSTRACT

MSc THESIS

SYNTHESIS OF COUMARIN-SCHIFF BASE DERIVATIVES AND INVESTIGATION PHOTOCHEMICAL PROPERTIES

Makki AZZAMAN

ÇUKUROVA UNIVERSITY
INSTITUTE OF NATURAL AND APPLIED SCIENCES
DEPARTMENT OF CHEMISTRY

Supervisor : Prof. Dr. Elife Sultan GİRAY
Year: 2022, Pages: 86
Jury : Prof. Dr. Elife Sultan GİRAY
Prof. Dr. Emel YILDIZ
Prof. Dr. Recep ÖZEN

Coumarins are a class of heterocyclic organic compounds consisting of oxygen, naturally exist in plants. They can be isolated from plants or synthesized in the laboratory. Coumarins have been known for possessing various biological activities along with the application in cosmetic, perfume and agricultural industries.

Schiff bases have become an essential class of chemical compounds that have been employed in both organic and inorganic chemistry. Schiff bases have been used as coloring agent and pigment as well as in pharmaceutical industry and as strong ligand due to the ability of forming complexes.

In this study, ten novel coumarin derivatives based on Schiff base were designed and synthesized. The study examined the photophysical properties for the new compounds in three different solvents to detect emission frequencies, Stokes shifts and the effect of solvents.

Key words: Coumarin, Schiff base, fluorophore, fluorescence activity, Stokes shift

ÖZ

YÜKSEK LİSANS TEZİ

KUMARİN-SCHİFF BAZI TÜREVLERİNİN SENTEZİ VE FOTOKİMYASAL ÖZELLİKLERİNİN ARAŞTIRILMASI

Makki AZZAMAN

ÇUKUROVA ÜNİVERSİTESİ
FEN BİLİMLERİ ENSTİTÜSÜ
KİMYA ANABİLİM DALI

Danışman : Prof. Dr. Elife Sultan GİRAY
Yıl: 2022, Sayfa: 86
Jüry : Prof. Dr. Elife Sultan GİRAY
Prof. Dr. Emel YILDIZ
Prof. Dr. Recep ÖZEN

Kumarinler, bitkilerde doğal olarak bulunan oksijen içeren heterosiklik organik bileşiklerin sınıfıdır. Kumarinler, bitkilerden izole edilebilir veya laboratuvarda sentezlenebilirler. Kumarinler, kozmetik, parfüm ve tarım endüstrilerinde kullanılmakta olup çeşitli biyolojik faaliyetlere sahip olarak bilinmektedir.

Schiff bazları, hem organik hem de anorganik kimyada kullanılan önemli bir kimyasal bileşik haline gelmiştir. Schiff bazları, renklendirici madde, pigment ve yanı sıra ilaç endüstrisinde, ayrıca kompleks oluşturma kabiliyeti nedeniyle güçlü ligand olarak kullanılmaktadır.

Bu çalışmada, schiff bazlarına dayalı on yeni kumarin türevi tasalanıp sentezlenmiştir. Çalışmada, emisyon frekanslarını, Stokes kaymalarını ve çözücü etkisini tespit etmek için üç farklı çözücüde yeni bileşiklerin fotokimyasal özellikleri incelenmiştir.

Anahtar kelımeler: kumarin, Schiff bazı, florofor, floresan aktivite, Stokes kayamsı

EXTENDED ABSTRACT

Fluorescence spectroscopy is a widely utilized method for the detection of activity of chemicals under UV-vis light. It has been used in chemistry, biology and medicine for decades and developing day by day. Fluorescence comes under luminescence which occurs when electrons gain energy through UV-vis lights to move from singlet ground state to singlet excited state, then electrons emit energy to stabilize and come back to the ground state. The transition of electrons from excited state to ground state could occur in two different ways: firstly, electrons move from the singlet excited state directly to the ground state emitting energy, this emission is called Fluorescence. The other option is electrons move to a triplet state and change spin direction then to the ground state emitting energy, this emission is called phosphorescence. Fluorescence is quite rapid, it occurs in 10^{-8} s, while phosphorescence takes longer to occur a consequence of the intersystem crossing stage and spin direction, it occurs in the range of 10^{-3} – 1 s. Luminescence can also be classified according to the source of energy. If the energy source is UV-vis light, then it is fluorescence or phosphorescence, if the energy source is bioreaction, then it is called bioluminescence, in case of chemical reaction as a source of energy, then it is called chemiluminescence, etc.

There are three types of fluorescence according to the amount of energy absorbed and emitted: 1. Stokes fluorescence when emission occurs at longer wavelength than absorption, 2. Anti-Stokes fluorescence takes place when emission occurs at shorter wavelength than absorption due to the exposure to external thermal energy, 3. Resonance fluorescence occurs only in crystals and gases but never in solutions, its emission energy equals absorption. The difference between emission and absorption frequencies is called Stokes shift.

A fluorescence spectrometer contains four major components: 1. Light source which is usually Xenon lamp, 2. Monochromator which provides the ability to choose the wavelength that passes through to the sample, 3. Sample holder which

is made of quartz, 4. Detector which changes the signal comes through a sample to electrical pulses.

Coumarins basically consist fused benzene and pyrone rings, it essentially can be found in plants but it can also be synthesized in laboratories. Coumarin derivative have been known for playing role in many industries and for the pharmaceutical and biological activities as anti-inflammatory, anti-viral, anti-oxidant,etc. coumarin derivatives are utilized as dye lasers and coloring agents for the reason they mostly exhibit fluorescence.

Several hundreds of coumarins in nature have been identified and classified based on the functional groups they are carrying. Coumarins classified to: simple coumarin, furanocoumarin, dihydrofuranocoumarin, pyranocoumarin, phenylcoumarin and bicoumarin. There are several methods for coumarin synthesis in the literature, such as Perkin, Pechmann, knovenagel, ponndorf methods, etc.

Shiff bases form when a condensation reaction occurs between an amine group with a carbonyl group on aldehydes or ketones, where the nitrogen forms double bond with the carbonyl carbon called imine. Schiff bases are utilized as coloring agent and they have pharmacological activities as anti-viral, anti-microbial and anti-fungal. Imines can be classified based upon the parent amine group to: 1. Formed from primary amines, 2. Formed from anilines 3. Formed from hydrazines which can form hydrazones, azines or oximes.

In this study, couamrin was synthesized via Pechmann reaction in the presence of amberlyst 15 as catalyst. The reaction yield was 92%. Then coumarin underwent through formylation reaction using hexamethylenetetramine and acetic acid as a reaction medium. The reaction yield was 15 %. As the third stage formylated coumarin was used to produce coumarin derivatives in two sets of reactions. First, in order to form coumarin-imine hybrids, anilines holding different substitutions were used to react with formylated coumarin, and **3a**,**3b**,**3c**,**3d** and **3e** were obtained. Second set of reactions was to form coumarin-hydrazone hybrids, different hydrazines were used to react with formylated coumarin, and **4a**,**4b**,**4c**,**4d**

and were obtained. Chemical structure of coumarin derivative were confirmed through IR and both ^{1}H NMR and ^{13}C NMR.

UV-vis absorption for coumarin derivatives were examined at the concentration of 10 μM in three different solvents: Dimethyl sulfoxide (DMSO), ethanol (EtOH) and acetonitrile (ACN). The investigation concluded to all fluorophores have relatively similar absorption maxima in each solvent. Absorption intensity increases in ACN. Absorption was red-shifted in DMSO comparing to EtOH and ACN.

Fluorescence emission and Stokes shift were investigated for coumarin derivatives. In DMSO, **3a** emitted at 472, **3b** at 468, **3c** at 471, **3d** at 478, **3e** at 456, **4a** at 416, **4b** at 438, **4c** at 440, **4d** at 456 and **4e** at 436 nm, Stokes shifts for **3a**= 124, **3b**= 120, **3c**= 126, **3d**= 132, **3e**= 110, **4a**= 86, **4b**= 90, **4c**= 92, **4d**= 114 and **4e**= 86 nm. In EtOH, 4a emitted at 340,**3b** at 338, **3c** at 340, **3d** at 336, **3e** at 354, **4a** at 338, **4b** at 338, **4c** at 338, **4d** at 446 and **4e** at 340 nm. Stokes shifts for **3a**= 110, **3b**= 110, **3c**= 110, **3d**= 100, **3e**= 121, **4a**= 110, **4b**= 110, **4c**= 108, **4d**= 214 and **4e**= 112 nm. In ACN, **3a** emitted at 338, **3b** at 364, **3c** at 370, **3d** at 362, **3e** at 366, **4a** at 364, **4b** at 368, **4c** at 364, **4d** at 371 and **4e** at 366 nm, Stokes shifts for **3a**= 130, **3b**= 72, **3c**= 78, **3d**= 64, **3e**= 66, **4a**= 66, **4b**= 76, **4c**= 66, **4d**= 76 and **4e**= 72. Stokes shifts in DMSO and EtOH can be considered as large Stokes shifts.

Fluorescence activity investigation in DMSO for coumarin derivatives in the study presented emission in visible range. Unlike in EtOH and ACN. 4d in EtOH exhibited excessively large Stokes shift and emitted in the visible range.

ACKNOWLEDGMENT

First, I thank and praise the Almighty for the mercies, grace and letting me through all the difficulties

I would like to express my warmest gratitude and thanks to my dear supervisor Prof.Dr. E. Sultan Giray for her support, patience and guidance throughout this research work despite her medical condition.

My thanks also go to Instructor Dr. Onur Demirkol, and Research Assistant and PhD student. Mehmet Erşatır, whom I benefited from their knowledge, skills and experience.

I would like to thank all the Chemistry department staff and friends at Çukurova University, who contributed to my thesis.

My deep thanks to all staff in Turkish Education Application and Research Center TÖMER, especially my dear Turkish language teacher Berrin Özcan for all the help she has provided throughout my stay in Turkiye.

Last but not least, I would like to express my endless thanks and gratitude to my whole dear family, especially my parents, brothers and sisters whom I have always felt their prayers along my side all the time, believed in me, supported me by all means, that I can never pay back. I also thank all my friends around the world.

CONTENTS **PAGE**

LIST OF TABLES **PAGE**

LIST OF FIGURES **PAGE**

SYMBOLS AND ABBREVIETIONS

s : Second

nm : Nano-meter

TLC : Thin layer chromatography

FT-IR : Infra-red

^{1}H NMR : Proton nuclear magnetic resonance

^{13}C NMR: C-13 nuclear magnetic resonance

UV-vis : Ultraviolet – visible light

h : Hours

^{o}C : Celsius degree

g : Gram

M.W. : Molecular weight

DMSO : Dimethyl sulfoxide

EtOH : Ethanol

ACN : Acetonitrile

$AlCl_3$: Aluminum chloride

$FeCl_3$: Ferric chloride

$ZnCl_2$: Zinc chloride

HCl : Hydrochloric acid

THF : Tetrahydrofuran

CO : Carbon monoxide

Pd : palladium

μM : Micromolar

λ_{Abs} : Maximum absorption wavelength

λ_{Em} : Maximum emission wavelength

$\Delta\lambda$: Stokes shift

1. INTRODUCTION

1.1. Fluorescence Spectroscopy

Fluorescence spectroscopy has been widely used in chemistry and biology in last four decades. It has become an indispensable tool in the medical field and natural sciences (Lakowicz, 2006a). The use of fluorescence has been growing rapidly throughout different discipline along with the meticulous development of light sources, detection parts and convenient devices (Valeur & Brochon, 2001).

1.1.1. Fluorescence Phenomena

Electronically excited states cause Luminescence, which can be defined as the emission of light from any substance. Based on the nature of excited state, luminescence is initially classified into two types: phosphorescence and fluorescence. The electrons in the ground state are paired by opposite spin (singlet state). When a photon with a specific wavelength excites an electron, the electron absorbs the energy and moves to a higher energy state, then rapid re-emission of the absorbed photon occurs allowing the electron to return to the ground state with no change in spin orientation during context. This phenomenon is called Fluorescence and the fluorescent substance is called Fluorophore. The typical emission rate of fluorescence is 10^{-8} s, which needs precise optics and electronic devices because of short timescale of fluorescence.

The phenomenon of phosphorescence on the other hand, occurs when the excited electron in the higher energy level, has spin direction as the other electron in the ground state (triplet state). Spin correspondence forbids excited electron transition to the ground state and delays emission to the rate of 10^{-3} – 10^{0} s. Phosphorescence involves intersystem transition from excited singlet to triplet state since transition from ground singlet state to triplet state is implausible because electrons have to possess lowest amount of energy possible to stay in the ground state and that can be achieved by spinning in the opposite orientation (Fig.1.1).

The amount of emitted energy in fluorescence or phosphorescence phenomenon is definitely lower than the absorbed energy during the excitation process. In other words, the wavelength of the absorbed energy is shorter than the emitted (Lakowicz, 2006; Guilbault, 1990).

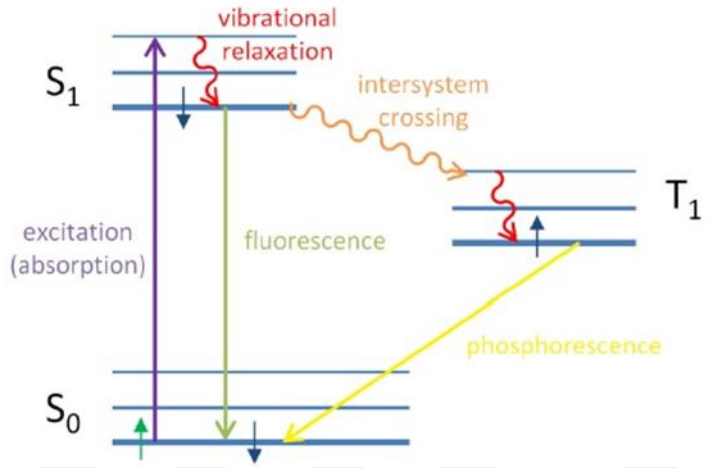

Figure 1.1. Jablonsky diagram showing the difference between fluorescence and phosphorescence (Eck, 2017).

There is another approach to classify luminescence according to the nature of the source of excitation energy. For instance, if the excitation energy is obtained from organisms, then it is called bioluminescence. If the excitation energy is produced by a chemical reaction, then it is called chemiluminescence. Thermoluminescence is caused by a substance with high energy levels releases energy at a temperature below redheat. The release of energy caused by cathode ray exposure causes cathodoluminescence. When certain crystals, such as sugar, are broken, triboluminescence (Greek tribo, to rub) is produced as a release of energy. The energy held during crystal forming is released as the crystal breaks (Guilbault, 1990). Types of luminescence summarized in Table 1.1.

Table 1.1. Different types of luminescence

S	Type of luminescence	Source of energy
1	Fluorescence	UV-visible light
2	Phosphorescence	UV-visible light
3	Bioluminescence	Biochemical reaction
4	Chemiluminescence	Chemical reaction
5	Thermoluminescence	Heat transmission
6	Cathodoluminescence	Cathode ray exposure
7	Triboluminescence	Crystal fission

1.1.2. Historical Review

The terms luminescence and phosphorescence are originated from (Latin lumin, light and Greek phosphor, to bear light) respectively. They both have light in the terms. In fact, the name phosphor has been given to substances that glow in the dark after an exposure to light. However, it is not the case with fluorescence. In 1852, Sir George Gabriel Stokes, a physicist and mathematics professor, did a simple experiment when he exposed a tube filled with a solution of quinine sulfate, to sunlight through a prism. He noticed that nothing had happen to the solution. It simply remained transparent. However, the solution glowed with a blue light when it was exposed to the spectrum beyond violet light at the non-visible region. Stokes published a paper with his observations and called the phenomenon (dispersive reflexion) and later on a following paper he used the term fluorescence (from fluorspar which is used for fluorite containing minerals), to describe the phenomenon. The word fluor (Latin fluere, to flow) refers to (spar, an English vocabulary used “stones” had been used in 1700s), these spars can melt easily. This is the origin of the name of the element Fluor.

In 1842, Edmond Becquerel, a physicist, published a paper on a similar experiment to Stokes’, where he exposed calcium sulfide to ultraviolet beam and calcium sulfide glowed. Further experiments were done to observe the difference

between fluorescence and phosphorescence and characterize them(Valeur & Brochon, 2001).

1.1.3. Types of Fluorescence

Fluorescence can be classified into three different types based on the amount of excitation and emission energy (Fig.1.2):

a. Stokes fluorescence: it is an emission of photons with longer wavelength than the absorbed photons. It is commonly observed in solutions.
b. Anti-Stokes fluorescence: it is an emission of photons with shorter wavelength than the absorbed photons., caused by the addition of thermal energy to an excited energy level. It is commonly seen in dilute gases at high temperatures.
c. Resonance fluorescence: it is an emission of photons with the same wavelength of the absorbed photons. It can be observed in crystals and gases but never in solutions. It is also called Rayleigh scattering(Guilbault, 1990).

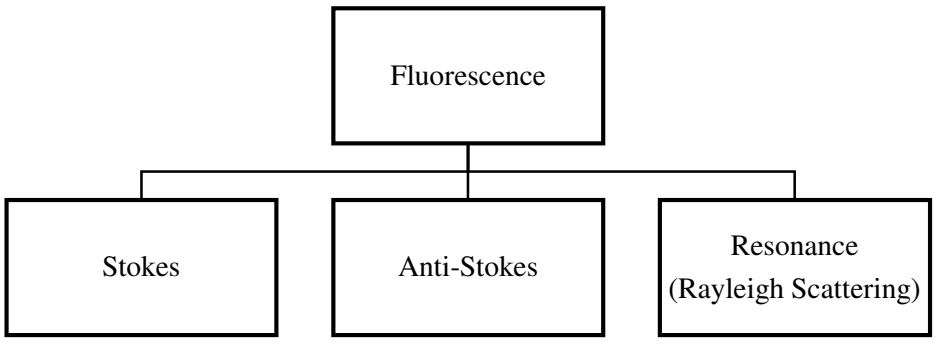

Figure 1.2. Types of Fluorescence (Munjanja & Sanganyado, 2015)

1.1.4. Stokes Shift

According to Jablonski diagram (Fig.1.1), it is obvious that the emitted energy is lower that the absorbed. When Sir George Gabriel Stokes performed his first fluorescent experiment, he noticed that the energy given to the sample was in the ultraviolet region which is shorter wavelength or higher energy (Fig.1.3) than the energy emitted by the fluorophore which was in visible light region meaning it is longer wavelength or lower energy (Lakowicz, 2006a).

As mentioned earlier, during excitation, an electron gains energy and migrates from the ground state to the excited state. Each electronic state is divided to sublevels representing vibrational movements of the molecules. The molecule immediately relaxes after excitation to the lowest sublevel of the excited electronic state which causes loss of energy as heat or vibrations resulting Stokes Shift.

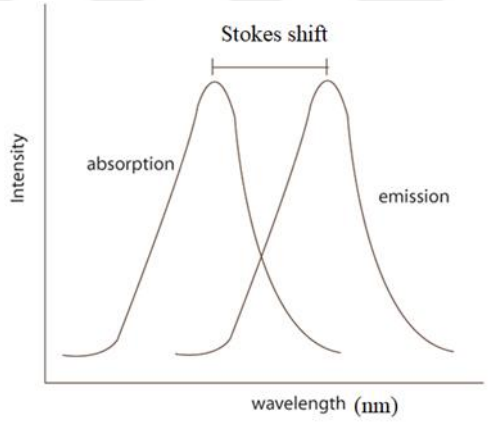

Figure 1.3. Stokes shift and the difference between absorbed and emitted energy wavelength

1.1.5. Fluorescence Instrumentation

Fluorescence instrument is principally used to measure the wavelength of the emitted energy from the fluorophore. Nonetheless, it is important for the instrument to have amount of energy selectable source, scattering minimizer, a detector, electronical device to process the data. Over the years, fluorescence

spectrometer has become more advanced and accurate (Fig.1.4). Here are the basic components of a fluorescence spectrometer:

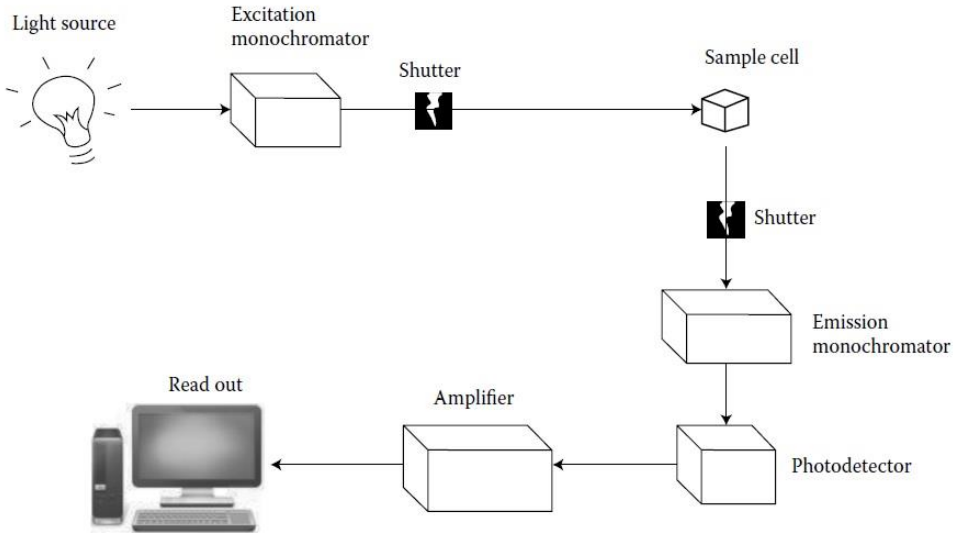

Figure 1.4. Schematic fluorescence spectrometer (Munjanja & Sanganyado, 2015)

1.1.5.1. Light Source

Most common light source is Xenon lamp. It can provide spectra in the range of 220 to 590 nm with 2000 h of half-life. Glass containers should not be used with Xenon lamp, because glass does not transmit energy shorter than 350 nm, instead quartz containers are advised to be used for pure energy transmission. There are other light sources can be used such as mercury lamp and mercury phosphor lamp.

1.1.5.2. Monochromators

Since the light carries a wide range of wavelength, there is need to a component that disperses light into various wavelengths. There comes the excitation monochromator to disperse the light and provide the ability to choose a specific wavelength for the sample to be exposed to. In order to reduce stray light, monochromator contains entrance and exit slits in addition to disperser part. There

is also an emission monochromator which is placed behind the sample cell to remove undesired wavelengths.

1.1.5.3. Sample Holder

Quartz or suprasil based sample holders should be used in fluorescence measurements.

1.1.5.4. Detector

The transmitted photons from the fluorophore sample moves through emission monochromator to a photomultiplier (PMT) which works as a detector and amplifies the signal and changes it to electrical pulses that can be shown on an programed electronical device(Jameson et al., 2003; Lakowicz, 2006; Munjanja & Sanganyado, 2015; Guilbault,1990).

1.2. Coumarin

Coumarins are basically found in many plants. The name coumarin comes after a French term of Tonka bean “Coumarou”, the plant which coumarin had been isolated from for the first time in 1820s. Coumarins consist of a pyrone ring attached to a benzene ring (Fig.1.5), which make them a member of the benzopyrone class of organic compound (Novak & Kovač, 2000). Coumarin derivatives have effective role in many industries, such as perfumes, cosmetics and agricultural field. They are also used widely in the pharmaceutical field showing numerous biological activities as neuroprotective, anti-inflammatory, anti-viral, anti-cancer, anti-oxidant, and other medical uses (Lingaraju et al., 2018; Matos et al., 2012; Pérez-Cruz et al., 2018; Tapanyiğit et al., 2020). Coumarin derivative mostly show intensive fluorescence activity in the UV-visible region which make them a good candidates as dye lasers, colorant and non-linear chromophores (Fylaktakidou et al., 2005; Ngoc Toan & Dinh Thanh, 2020). Many scientists have suggested the chemical formula of coumarin,

thus, the suggested formula by Strecker (1867), Fittig (1868) and Tiemann (1877), has been considered to be the correct one (Fig.1.5) (Suresk M. Sethna & Shah, 1945).

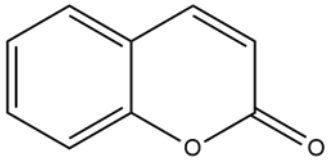

Figure 1.5. Chemical structure of coumarin

1.2.1. Coumarin Classification

Coumarin and derivatives have been considered as a class of natural chemicals found throughout nature around the globe. Several hundreds of coumarin have been identified in nature. There are 6 classifications of coumarin (Fig.1.6).

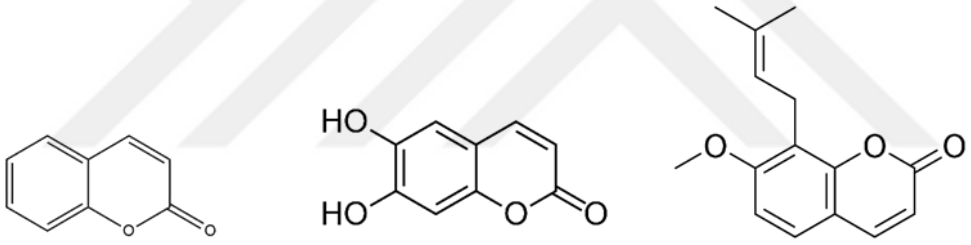

Coumarin *Esculetin* *Osthole*

a. Simple coumarin

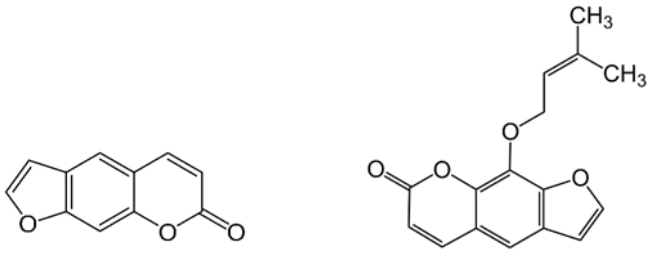

Psoralen Imperatorin

b. Furanocoumarin

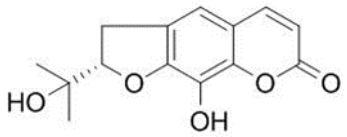

Rutaretin

c. Dihydrofuranocoumarin

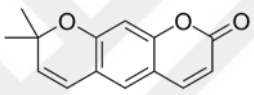

linear type: Xanthyletin

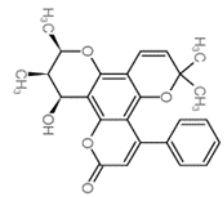

Angular type: Inophyllum A

d. Pyranocoumarin

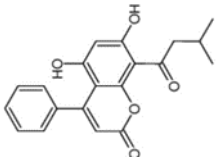

Isodispar B

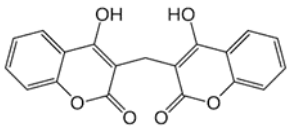

Dicoumarol

e. Phenylcoumarin f. Bicoumarin

Figure 1.6. Examples of coumarins

1.2.2. Coumarin Synthesis

Forasmuch there is considerable variety of coumarin derivatives, it caught scientists' eyes to synthesize coumarin derivatives in the laboratories. This interest led to numerous practical methods of coumarin derivatives synthesis. It is worth

mentioning that the most important step in coumarin synthesis though almost all the methods, is pyrone ring formation. Then different functional groups can be attached to the synthesized coumarin. Some of these methods were listed below.

1.2.2.1. Perkin Coumarin Synthesis

The first one to synthesize coumarin was performed by Perkin in 1868, via heating salicylaldehyde with acetic anhydride and anhydrous sodium acetate. (Fig 1.7).

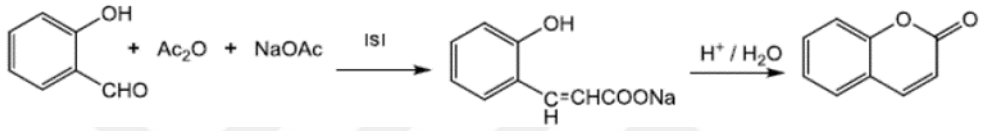

Figure 1.7. Perkin coumarin synthesis reaction (Sethna & Shah, 1944).

1.2.2.2. Pechmann Coumarin Synthesis

In this coumarin synthesis reaction, phenols and acetoacetic esters are used in presence of sulphuric acid at 100-120 ^{o}C. This coumarin product in this reaction carries a substituent on each benzene and pyrone rings (Von Pechmann & Duisberg, 1883). Many other acidic catalysts can be used rather than sulphuric acid such as amberlyst 15 (Hoefnagel et al., 1995; Hussien et al., 2016), $AlCl_3$ (Sethna et al, 1938), $FeCl_3$ (Kumar et al., 2008), $ZnCl_2$ (Corrie, 1990). (Fig.1.8; Fig.1.9).

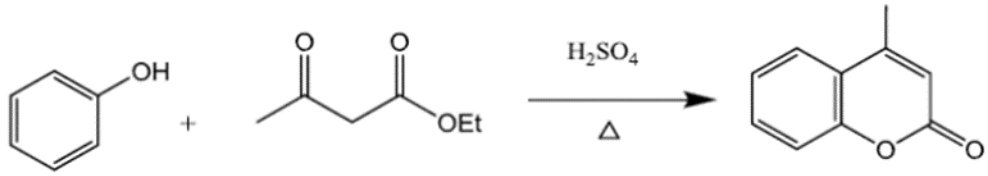

Figure 1.8. Pechmann coumarin synthesis reaction

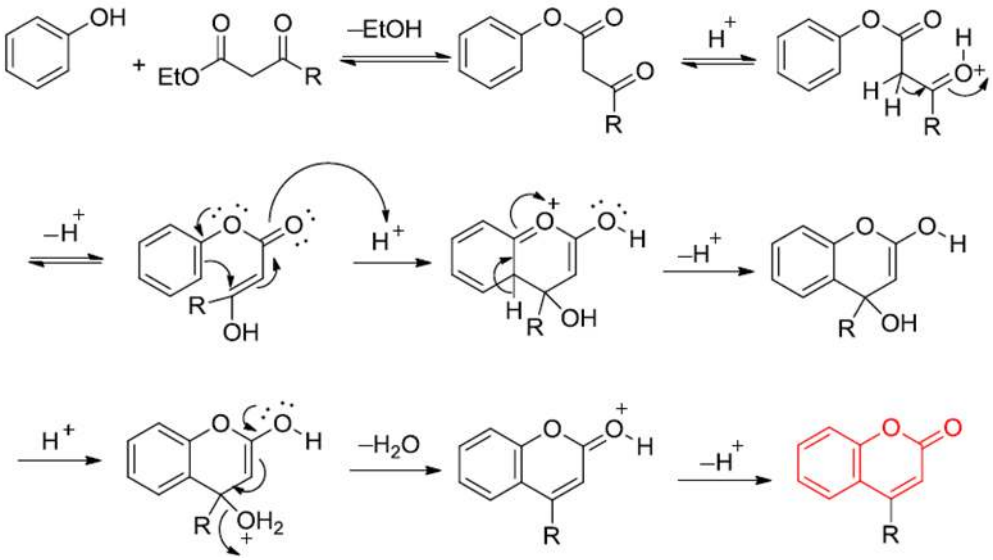

Figure 1.9. General Pechmann reaction mechanism

1.2.2.3. Coumarin Synthesis by Using Terminal Alkynes With Catalytic Palladium

Coumarin can be produced by reacting *o*-iodophenol with phenylacetylene under CO in the presence of Pd as catalyst (Fig.1.10) (Kadnikov & Larock, 2003).

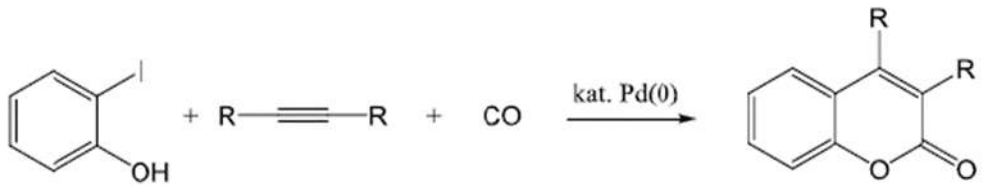

Figure 1.10. Synthesis of coumarin from terminal alkyne using catalytic palladium

1.2.2.4. Knoevenagel Coumarin Synthesis

In 1890, Knoevenagel developed a coumarin synthesis method using o-hydroxybenzaldehyde and β-keto esters or malonates in the presence of an organic base such as pyridine, pipyridine and amberlyst 26 (Fig.1.11) (Erşatır et al, 2016; Knovenagel,1898; Sethna & Shah, 1944; List & Turberg 2019).

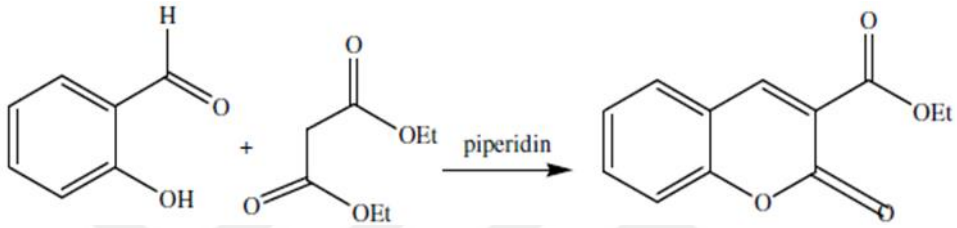

Figure 1.11. Knoevenagel coumarin synthesis reaction

12.2.5. Synthesis of Coumarin Through Wittig Condensation Reaction

This method is a condensation reaction occurs between an aldehyde or a ketone with triphenylphosphonium ylide in order to form an alkene (Heravi et al., 2020). The wittig reaction was modified and utilized to produce coumarin starting with salicylaldehyde (Fig.1.12) (Harayama et al., 1991; Narasimhan et al., 1979).

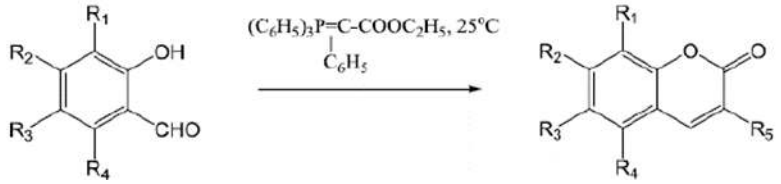

Figure 1.12. Wittig coumarin synthesis

1.2.2.6. Ponndorf Coumarin Synthesis

Cinnamic acid with phenol or substituted phenol was used to form coumarin in acidic medium. The method can be used in all coumarin synthesis generally (Fig.1.13) (Simpson & Stephen, 1956)

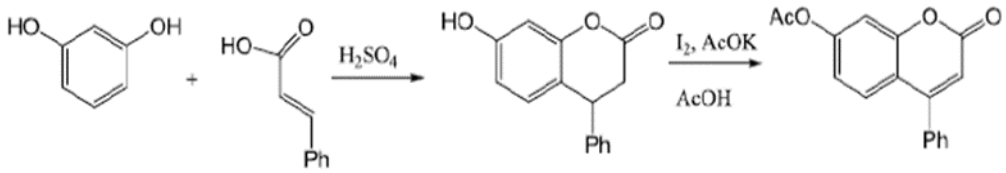

Figure 1.13. Ponndorf coumarin synthesis reaction

1.2.2.7. Synthesis of Coumarin via Houben-Hoesch Reaction

In the presence of both of Lewis acid and HCl, organic nitriles react with electron-rich phenols to form coumarin (Fig1.14.) (Bargellini & Forti, 1911; Hoesch, 1915).

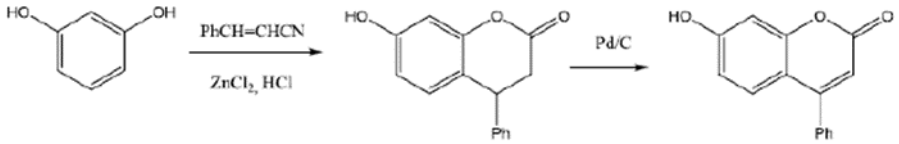

Figure 1.14. Houben-Hoesch coumarin synthesis reaction

1.2.2.8. Allan-Robinson Coumarin Synthesis

When aromatic anhydrides were used for the acylation of *o*-hydroxyaryl ketones followed by cyclization, flavones can be formed, however, in case of using aliphatic anhydrides rather than aromatic anhydride, coumarin can be formed (Fig.1.15) (Kostanecki & Rozycki, 1901).

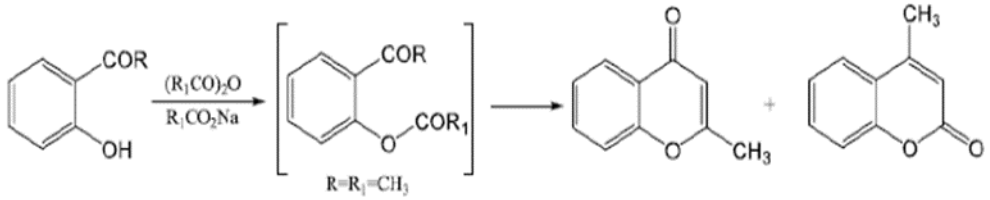

Figure 1.15. Allan-Robinson coumarin synthesis reaction

1.3. Schiff Bases

Schiff base is a widely used and a common term in chemistry. It is basically composed when a primary amine group reacts with a carbonyl group on an aldehyde or ketone, where the nitrogen from the amine group forms a double bond called (imine), with the carbon on the carbonyl group forming Schiff base. It was synthesized for the first time in 1864 by Hugo Schiff (Schiff, 1869). Schiff bases have pharmacologic properties such as anti-fungal, anti- cancer, anti-microbial, anti-viral (Ashoor et al., 2020). They are also used in pigments and coloring agents as well as Schiff bases are widely used as ligands in inorganic chemistry.

1.3.1. General reaction mechanism of Schiff base (imine) formation

Imine can be formed as a result of the reaction between ammonia or a primary amine with a carbonyl group on aldehydes or ketones (Fig.1.16; Fig.1.17). The reaction usually takes place in catalytic amount of acids. Simple Schiff bases hydrolize easily, unlike Schiff bases formed from aromatic aldehydes or ketones. They are relatively more stable.

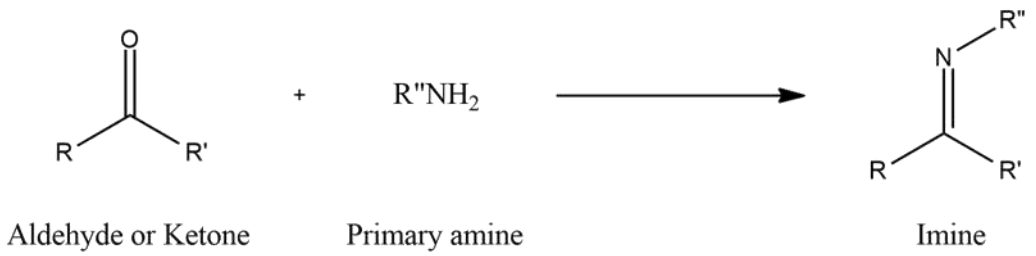

Figure 1.16. General reaction of Imine formation

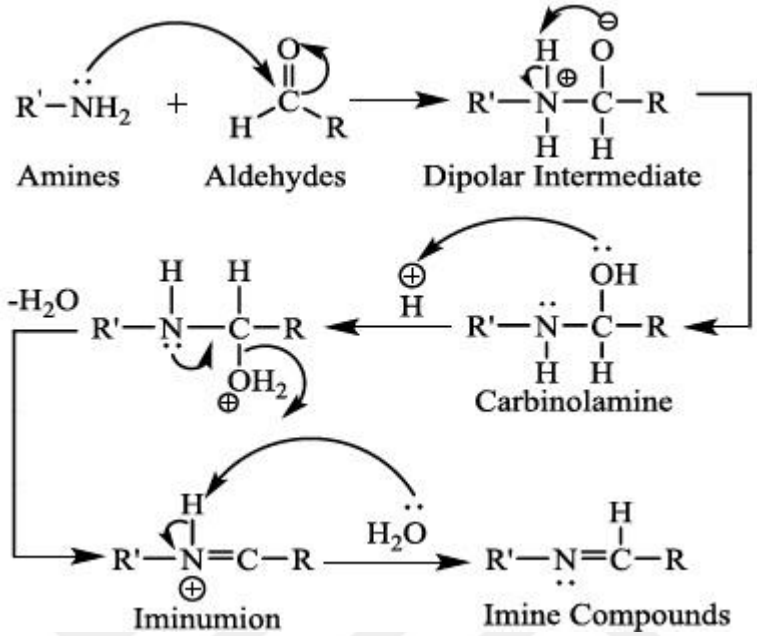

Figure 1.17. Imine formation proposed mechanism

1.3.2. Classification of Imines

Imines can be formed from expanded variety of carbonyl group holders and amines. Due to that diversity of imine formation probability, it is possible to classify imines according the parent amine group. Some of derived imines from different amines were listed below (Fig.1.18; Fig.1.19) (Forman, 1964; Dayagi & Degani, 1970).

1.3.2.1. Imines formed from primary amines

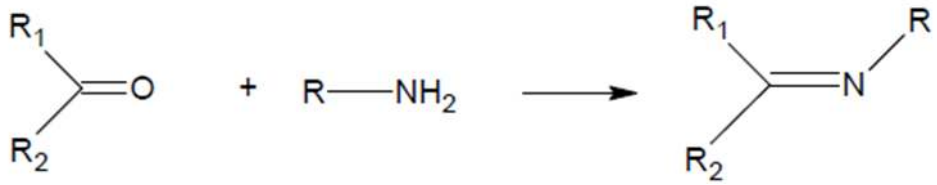

Figure 1.18. Imine formed from primary amine

1.3.2.2. Imines formed from anilines

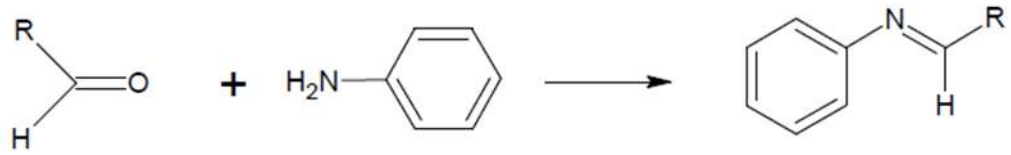

Figure 1.19. imine formed from aniline

1.3.2.3. Imines formed from hydrazine

The reaction between carbonyl group on aldehydes or ketones with unsubstituted hydrazine produces either hydrazones or azines depending on stoichiometry and reaction conditions (Fig.1.20; Fig.1.21; Fig.1.22).

a. Hydrazones

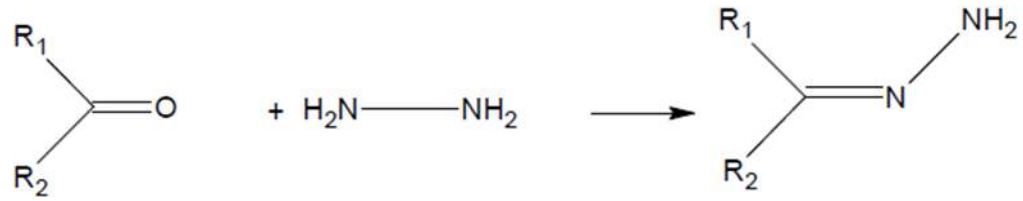

Figure 1.20. Imine formation from Hydrazine (Hydrazone)

b. Azines

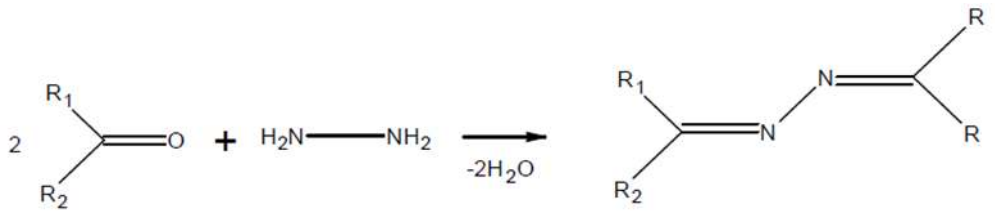

Figure 1.21. Imine formation from Hydrazine (Azine)

1.3.2.4. Imines formed from hydroxyl amines (oximes)

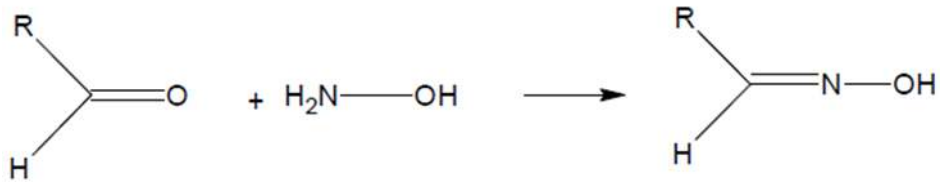

Figure 1.22. Imine formation from hydroxyl amine

1.4. Purpose of Study

This thesis aimed to design and synthesize novel different coumarin derivatives possessing large Stokes shifts, based on primary amines and hydrazines carrying various functional groups, linked to C-8 on 7-hydroxy-4-methyl-2H-chromen-2-one. The study worked on the confirmation of the chemical structure then investigated the photophysical properties of the coumarin derivatives, and the interaction between the products and different organic solvents, compared among the results and concluded with suggestions for further studies.

2. LITERATURE REVIEW

Due to low cost, easy manufacturing and the instability of Schiff bases in water, Coumarin-imine based fluorophores were designed and synthesized (Fig.2.1) (W. Y. Kim et al., 2016).

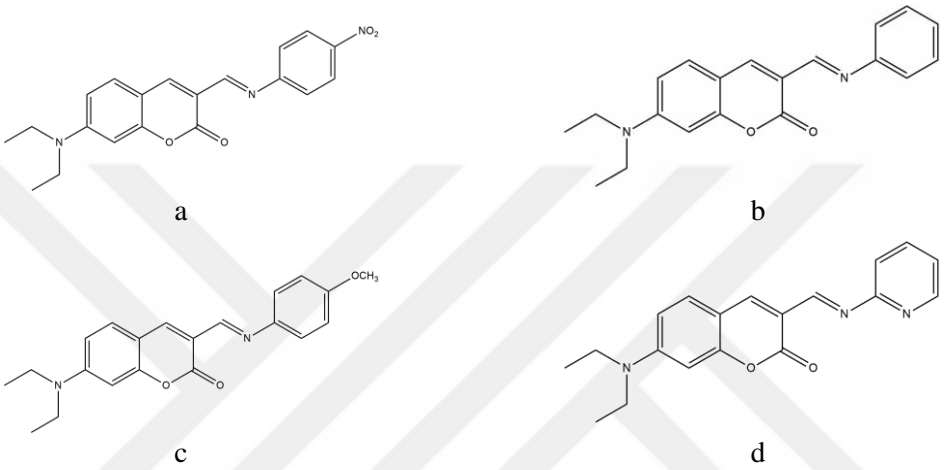

Figure 2.1. Fluorophores synthesized by (W. Y. Kim et al., 2016)

Fluorescence activities of the products were examined in different organic solvents at 10 μM for each. It was found that all the compounds are stable in organic solvent, however, they are sensitive to moisture. The study of fluorescence emission showed that B and D have shown blue shift during the hydrolysis while A has shown red shift upon hydrolysis. It also showed that the hydrolysis of B and D was extraordinarily boosted in acidic media. The study concluded by proposing that D can be a fluorescent potential moisture sensor at different pH values for the reason that the nitrogen on the pyridine ring could form hydrogen bonds which in turn can accelerate the hydrolysis process.

Shirashi et al., synthesized a chemical sensor for hypochlorous acid (HClO) which is secreted as anti-viral and anti-bacterial into human body immune system. It is also extensively utilized in water disinfection and hygiene supplies. An excess

amount of HClO could cause serious issues on human and animals health. The synthesized based chemical sensor was combined from 8-formyl-7-hydroxyl-4-methylcoumarin and 1,8-diaminonaphthalene. As shown in Fig.2.2 dehydrogenation occurs which leads to chemical shift from 7.0 to 7.1 on ^{1}H NMR diagram when exposed to HClO. The molecule undergoes rearrangement and forms imine bond which exhibits displays significant fluorescence. The study found that the sensor is efficient in 1% or more HClO and it does not exhibit fluorescence activity in acidic or basic media (Shiraishi et al., 2019).

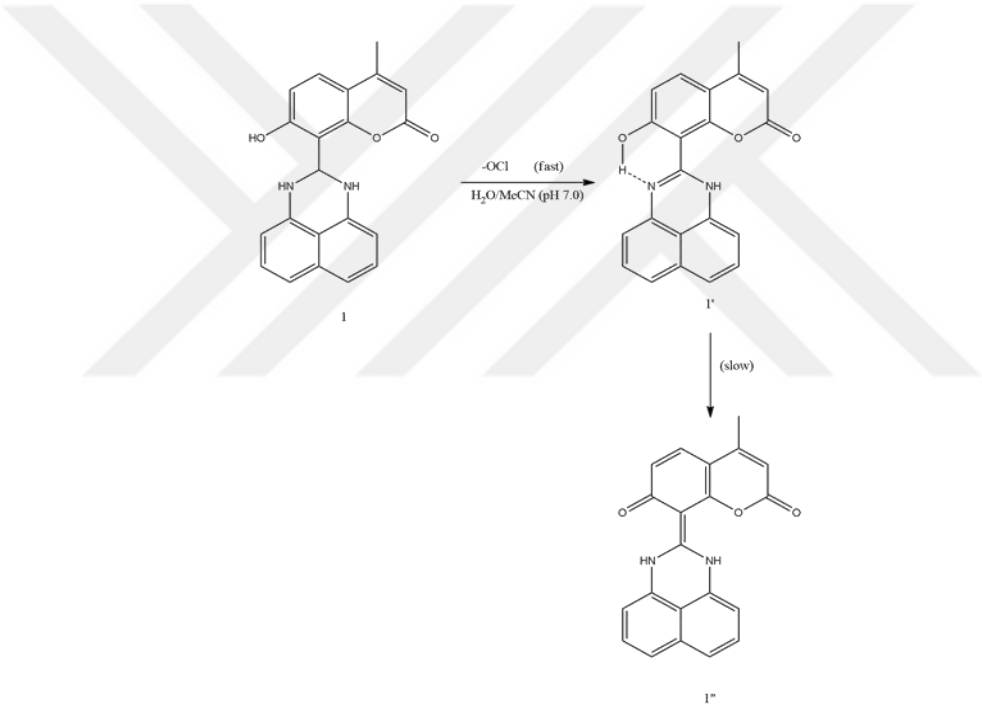

Figure 2.2. Coumarin based chemo sensor and its response to HClO (Shiraishi et al., 2019)

Shiraishi et al., succeeded to design and synthesize a highly sensitive to Cyanide ion (^{-}CN) sensor. The sensor is based on coumarin-imine and works by the Strecker reaction which can be described basically as a reaction between imine and hydrogen cyanide (HCN) to form α-amino nitriles (Shiraishi et al., 2016).

The obtained coumarin-imine hybrid was the product of the condensation of 8-formyl-7-hydroxy-4-methylcoumarin with 6-aminoquinoxaline. The product showed weak green fluorescence while when reacted with HCN and formed α-amino nitrile, it showed strong blue fluorescence (Fig.2.3).

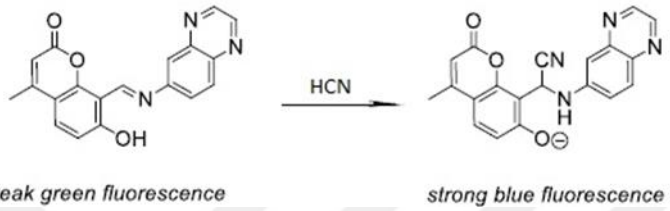

Figure 2.3. Effect of HCN on coumarin-imine based sensor (Shiraishi et al., 2016)

The study aimed for the sensor to effectively detect $^{-}$CN at low concentrations in neutral media due to the toxicity of HCN and the harm it causes to the human body and the environment.

Kulkarni et al., synthesized novel coumarin-imine based ligands (Fig.2.4). It was found that some of the complexes of these synthesized ligands has biological effect against some bacteria higher than regularly used drugs. Complexes of the ligands also showed significant outcome against most types of fungi, better than the outcome of some of the regularly used drugs. The ligands simply cleave the genome of bacteria and fungi in order to prevent them from growing. Possessing nitrogen and oxygen bey the ligands, gives them the capacity of being utilized as enzyme inhibitors (Kulkarni et al., 2008).

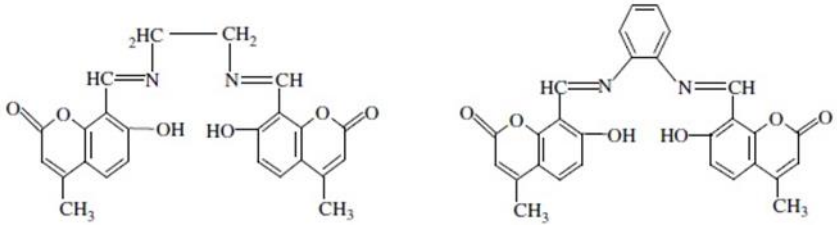

Figure 2.4. Coumarin-imine based ligands (Kulkarni et al., 2008)

Mahapatra et al., tried a new approach to synthesize a colorimetric receptor for diverse anion detection. In the study, a new coumarin-hydrazone sensor (Fig.2.5) was synthesized and investigated via ^{1}H NMR, UV-VIS and fluorescence spectroscopy (Mahapatra et al., 2011).

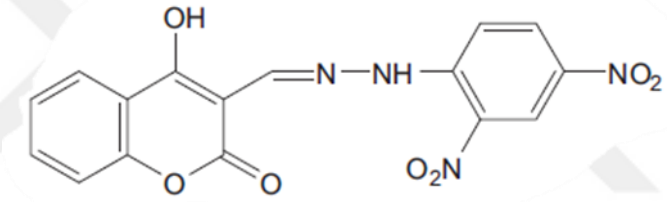

Figure 2.5. Synthesized coumarin-hydrazone sensor (Mahapatra et al., 2011)

The response of synthesized coumarin-hydrazone, to variety of anions such as AcO^-, $H_2PO_4^-$, HSO_4^- and halides, was investigated in 1:1 acetonitrile-water medium. Instant color changes occur on the solution especially in the presence of AcO^- ion. Yet, as fluorescence activity, synthesized coumarin-hydrazone sensor showed higher sensitivity to iodide among the anions considered.

Kim et al., developed an optical system based on hydrazone-acetate complexes for water content determination in acetonitrile (ACN) and tetrahydrofuran (THF). A comparison between two hydrazone-acetate complexes - anthracene based 1 and coumarin based 2 hydrazones was performed (Fig.2.6) (Kim et al., 2012).

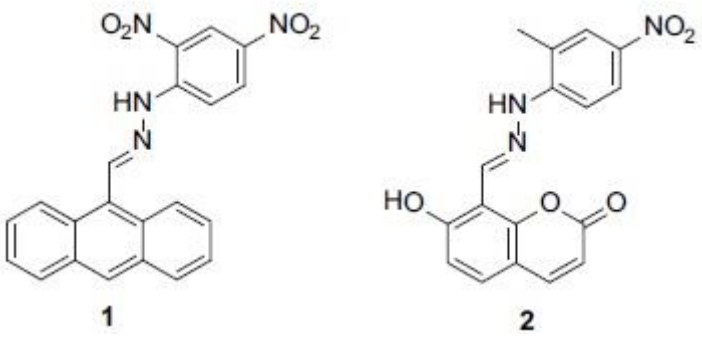

Figure 2.6. 1- Anthracene based hydrazine 2- Coumarin based hydrazone (Kim et al., 2012)

In terms of the stoichiometry of the hydrazone and the acetate is 1:1, it was found that 1-OAc responds effectively to water content in ACN and THF with an estimated limit of detection to be 0.037% and 0.071% respectively, while 2-OAc is relatively less sensitive to water content in ACN and THF, than 1-OAc, with 0.12% estimated detection limit. The changes occur on the color level of the solutions that can be seen by naked eye as well as changes in UV-vis absorbance. The study showed that as the concentration of the acetate increases the sensitivity of the complexes decreases.

The study concluded to that 1-OAc and 2-OAc can be utilized in up to 1-2% water content detection in ACN and THF, respectively. Though it emphasizes that 1-OAc is more sensitive than 2-OAc according to the data.

As fluoride has been used in daily life, fixed trace of it, is essential for human body, however, high amounts of it can be severely harmful. Thus, fluoride takes a large area in research and industry field. A new sensor based on coumarin-hydrazone was designed and synthesized (Fig.2.7). The sensor's synergy was investigated through UV-vis spectroscopy in the presence of AcO^-, NO_3^-, $H_2PO_4^-$, HSO_4^- and halides. It clearly exhibited color change only with fluoride present (Fig.2.8) (Zhuang et al., 2011).

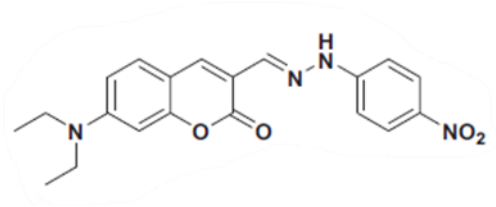

Figure 2.7. Fluoride ion sensor (Zhuang et al., 2011)

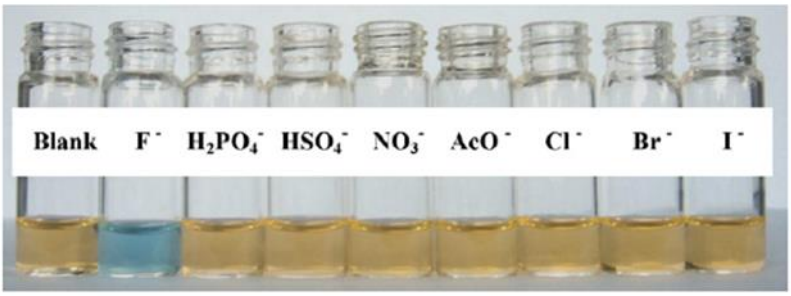

Figure 2.8. Synthesized sensor's interaction only with fluoride anion among other anions (Zhuang et al., 2011)

3. MATERIALS AND METHODS

3.1. Materials

3.1.1. Chemicals

- Ethanol
- Methanol
- Acetonitrile
- Dimethyl sulfoxide
- Resorcinol
- Ethyl acetoacetate
- Abmerlyst-15
- Hexamethylenetetramine
- Acetic acid glacial
- Hydrochloric acid (37%)
- Diethyl ether
- 2-aminophenol
- 3-bromoaniline
- 3-chloroaniline
- Aniline
- 2-amino-3-methylpyridine
- 2,4-dinitrophenylhydrazine
- Phenylhydrazine
- Methylhydrazine
- 2-hydrazinopyridine
- Hydrazine hydrate (80%)

3.1.2. Instrumentation

3.1.2.1. Chemical Structure Confirmation

- Thin layer chromatography TLC

  TLC was used to follow to progression of the reactions, to confirm that the reactants are completely transformed and to check the purity of the products. Dissolved sample was dripped onto Merck 60 F254 silica gel precoated aluminium sheet 25 mm thick, then the sheet was dipped into convenient mixture of solvents and exposed to Analytikjena UV lamp with dual wavelengths 254/365 nm.

- FT-IR

  In order to identify the functional groups on the synthesized products, IR spectra have been measured for a small amount of the product on the quartz lens of Thermo Scientific NICOLET iS10 spectrometer.

- ^{1}H NMR and ^{13}C NMR

  ^{1}H and ^{13}C NMR were recorded in $DMSO_4$-d_6: δH 2.25; δC 39.51 and $CDCl_3$ at 7.27 ppm for ^{1}H and 77.00 ppm for ^{13}C, on a Bruker Avance III 400 MHz spectrometer operating at 400 and 100 MHz respectively. All chemical shift values are represented in ppm and coupling constants represented in Hz. Multiplicities are elucidated, s (singlet), d (doublet), t (triplet) and m (multiplet). This procedure was done in Advanced Technology Education Research and Application Center at Mersin University.

3.1.2.2. Determination of Physical and Photophysical Characteristics

- Melting point measurement device

Capillary tubes were filled with product powder up to 50mm and put into Electrothermal 9100. Melting points were identified by gradual heating.

- UV-vis Absorbance

  Shimadzu UV 2101PC spectrophotometer was utilized to record the UV-vis absorbance in the range of 190-900 nm, for the synthesized products.

- Fluorescence properties

  Fluorescence assay was carried out in the Central Research Laboratory at Çukurova University using Cary Eclipse in a range of 250-400 nm for excitation and 360-1000 nm for emission.

3.2. Methods

Synthesis procedure consists of three stages

- ❖ 7-hydroxy-4-methylcoumarin synthesis.
- ❖ 8-formyl-7-hydroxy-4-methylcoumarin synthesis.
- ❖ Synthesis of Schiff bases (imines) and hydrazones derivatives of coumarins.

3.2.1. Synthesis of 7-hydroxy-4-methyl-2H-chromen-2-one (1)

Amberlyst-15 (0.24g, 10% of total weight of reactants) and ethyl acetoacetate (10 mmol 1.27 ml) were added into a two-neck flask, stirred for 5 minutes on a magnetic stirrer then resorcinol (10 mmol 1.1 g) was added to the mixture. The new mixture was heated up to 110-120 ºC for 60 minutes under a condenser (Fig.3.1). A solid white product was formed. It was dissolved in boiling methanol to recrystallize and remove amberlyst-15, then filtered rapidly. The filtrate was left aside in a well-ventilated dry area for the methanol to evaporate leaving a solid white product of 7-hydroxy-4-methyl-2H-chromen-2-one (**1**).

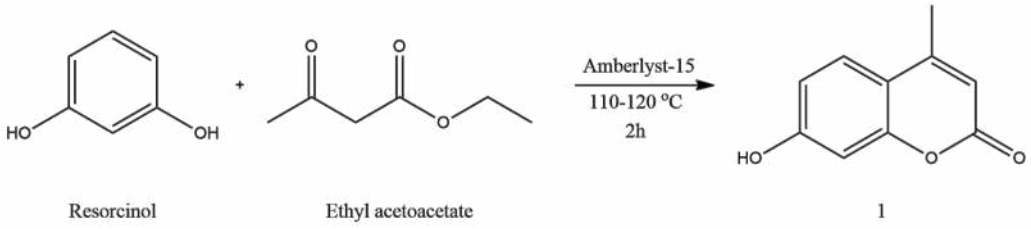

Figure 3.1. Synthesis of 7-hydroxy-4-methyl-2H-chromen-2-one (**1**)

White crystal, Yield: 92%

M.W.: 176.17 g/mol.

Melting point: 181-183 °C.

IR υmax (cm^{-1}): 3121 (O-H), 3070 (C-H) aromatic, 2807 (C-H), 1672 (C=O), 1583 & 1556 (C=C), 1130 (C-O)

δH (400 MHz, $DMSO_4$-d_6) 10.54 (s, 1H), 7.58 (d, J=8.4 Hz, 1H), 6.82 (dd, J_1=8.4 Hz, J_2=2.4 Hz, 1H), 6.72 (d, J= 2.4 Hz, 1H), 6.12 (s, 1H), 2.37 (s, 3H);

δC (100 MHz, $DMSO_4$-d_6) 161.13, 160.27, 154.83, 153.42, 126.49, 112.83, 112.00, 110.23, 102.17, 18.03.

3.2.2. Synthesis of 7-hydroxy-4-methyl-2-oxo-2H-chromene-8-carbaldehyde (2)

Synthesized **1** (90 mmol 15.9 g) is put into a flask along with hexamethylenetetramine (209.97 mol 29.43 g) and acetic acid glacial (150 ml). the mixture was heated under a condenser up to 70-80 °C for 5h in a water bath. The reaction was monitored by thin layer chromatography TLC in 4:1 ethyl acetate/hexane. Then 20% HCl was added and kept heated for another 30 min (Fig.3.2), cooled to room temperature and extracted by diethyl ether. A solid pale-yellow product 7-hydroxy-4-methyl-2-oxo-2H-chromene-8-carbaldehyde (**2**) is obtained after evaporation of solvent.

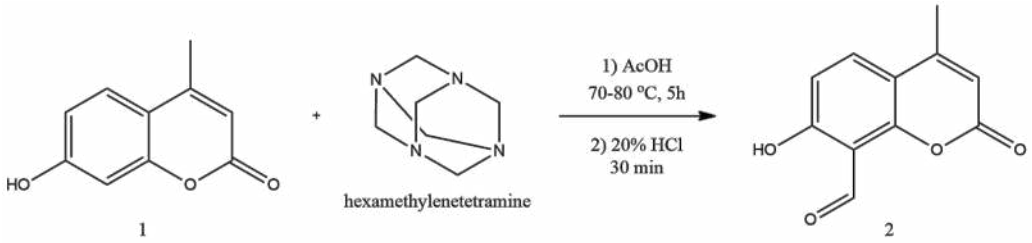

Figure 3.2. Synthesis of 7-hydroxy-4-methyl-2-oxo-2H-chromene-8-carbaldehyde (**2**)

Pale yellow crystal, yield: 15%

M.W.: 204.18 g/mol

Melting point: 175-176 °C.

IR υmax (cm^{-1}): 3399 (O-H), 3039 (C-H) aromatic, 2798 (C-H) aldehyde, 1728 (C=O) keton, 1678 (C=O) aldehyde, 1625 & 1589 (C=C), 1151 (C-O)

δH (400 MHz, $DMSO_4$-d_6) 11.88 (s, 1H), 10.40 (s, 1H), 7.89 (d, J=9.2 Hz, 1H), 6.93 (d, J=9.2 Hz, 1H), 6.27 (s, 1H), 2.39 (s, 3H);

δC (100 MHz, $DMSO_4$-d_6) 191.30, 163.68, 158.72, 155.12, 153.51, 133.26, 113.54, 111.82, 111.10, 108.95, 18.29.

3.2.3. General procedure for the synthesis of coumarin-imine hybrids (Schiff base formation)

2 and substituted aniline were added with ethanol as solvent into a flask, refluxed for 3-6 h (Fig.3.3) and monitored by thin layer chromatography TLC in 2:1 ethyl acetate/hexane. The mixture was cooled to room temperature, then filtered and washed out the residue for 3 times with ethanol. Solid product is obtained.

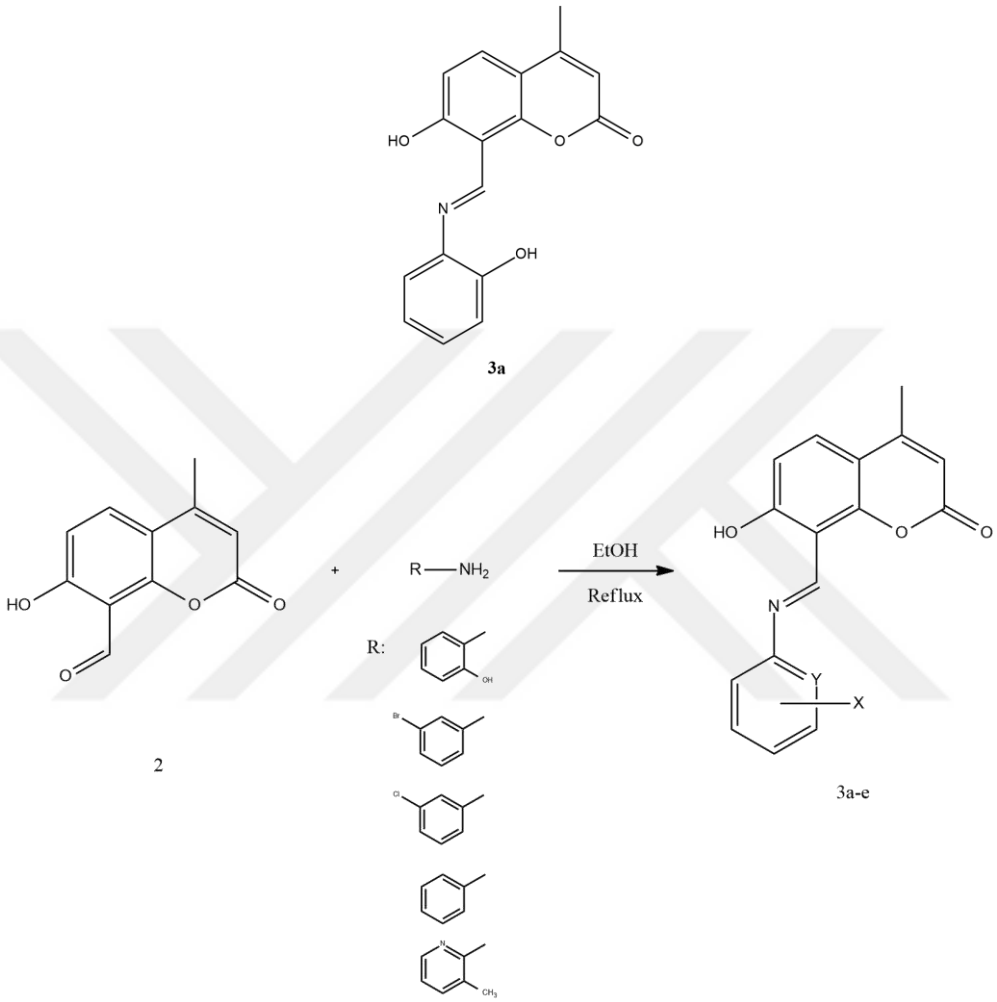

Figure 3.3. General synthesis procedure of coumarin-imine hybrids

3.2.3.1. (E)-7-hydroxy-8-(((2-hydroxyphenyl)imino)methyl)-4-methyl-2H-chromen-2-one (3a)

Orange color crystal; Yield: 90%

M.W.: 295.29 g/mol

Melting point: decomposed at 232 ºC

IR υmax (cm^{-1}): 3145 (O-H), 3036 (N-H), 1731 (C=O), 1621 & 1577 (C=C), 1609 (C=N), 1201 (C-N), 1157 (C-O)

δH (400 MHz, $DMSO_4$-d_6) 11.88 (s, 1H), 15.89 (s, 1H), 10.35 (s, 1H), 9.25 (s, 1H), 7.63 (d, J=8.8 Hz, 1H), 7.55 (d, J=8.8 Hz, 1H), 7.18 (t, J=7.2 Hz, 1H), 7.05 (d, J= 8.4 Hz, 1H), 6.93 (t, J=7.2 Hz, 1H), 6.72 (d, J=8.4 Hz, 1H), 6.10 (s, 1H), 2.34 (s, 3H);

δC (100 MHz, $DMSO_4$-d_6) 169.87, 159.27, 154.49, 154.00, 153.35, 150.52, 130.33, 128.68, 119.81,119.50, 116.58, 116.12, 109.24, 109.01, 105.73, 18.33.

3.2.3.2. (E)-8-(((3-bromophenyl)imino)methyl)-7-hydroxy-4-methyl-2H-chromen-2-one (3b)

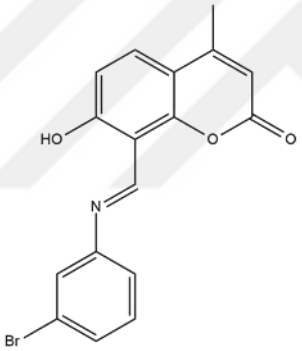

3b

Yellow crystal; yield: 87%

M.W.: 358.19 g/mol

Melting point: 170-172 °C.

IR υmax (cm^{-1}): 3059 (O-H), 2985 (N-H), 2967 (C-H), 1719 (C=O), 1627 (C=N), 1606 & 1559 (C=C), 1181 (C-N), 1074 (C-O), 769 (C-Br)

δH (400 MHz, $DMSO_4$-d_6) 14.40 (s, 1H), 9.16 (s, 1H), 7.76 (d, J=8.8 Hz, 1H), 7.73 (s, 1H), 7.53 (d, J=7.2 Hz, 1H), 7.48-7.40 (m, 2H), 6.90 (d, J= 8.8 Hz, 1H), 6.22 (s, 1H), 2.38 (s, 3H);

δC (100 MHz, $DMSO_4$-d_6) 164.77, 158.96, 158.33, 154.04, 153.79, 148.44, 131.35, 130.68, 130.06, 124.08, 122.35, 120.85, 113.92, 111.13, 110.57, 106.19, 18.30.

3.2.3.3. (E)-8-(((3-chlorophenyl)imino)methyl)-7-hydroxy-4-methyl-2H-chromen-2-one (3c)

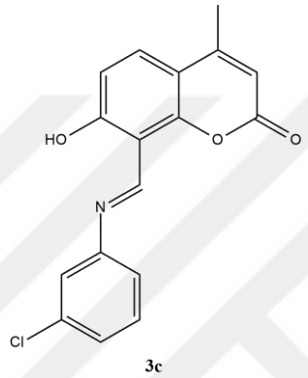

3c

Brownish green crystal, yield: 78%

M.W.: 313.74 g/mol

Melting point: 159-160 ºC.

IR υmax (cm^{-1}): 3089 (O-H), 3065 (N-H), 2988 (C-H), 1722 (C=O), 1648 (C=N), 1618 & 1565 (C=C), 1160 (C-N), 1071 (C-O), 772 (C-Cl)

δH (400 MHz, $DMSO_4$-d_6) 14.37 (s, 1H), 9.10 (s, 1H), 7.70 (d, J=8.8 Hz, 1H), 7.54 (s, 1H), 7.46 (d, J=7.2 Hz, 1H), 7.40-7.37 (m, 2H), 6.84 (d, J= 8.8 Hz, 1H), 6.18 (s, 1H), 2.36 (s, 3H);

δC (100 MHz, $DMSO_4$-d_6) 164.73, 158.89, 158.11, 153.95, 153.65, 148.20, 133.98, 131.03, 130.56, 127.14, 121.26, 120.33, 113.86, 111.06, 110.54, 106.12, 18.26.

3.2.3.4. (E)-7-hydroxy-4-methyl-8-((phenylimino)methyl)-2H-chromen-2-one (3d)

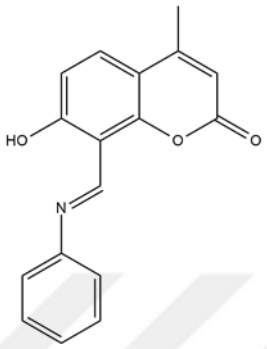

3d

Orange color crystal, yield: 67%

M.W.: 279.29 g/mol

Melting point: 160-162 ºC.

IR υmax (cm^{-1}): 3083 (O-H), 3056 (N-H), 2938 (C-H), 1731 (C=O), 1658 (C=N), 1615 & 1571 (C=C), 1163 (C-N), 1075 (C-O)

δH (400 MHz, $DMSO_4$-d_6) 14.89 (s, 1H), 9.17 (s, 1H), 7.75 (d, J=9.2 Hz, 1H), 7.52-7.47 (m, 4H), 7.39-7.36 (m, 1H), 6.89 (d, J= 9.2 Hz, 1H), 6.21 (s, 1H), 2.38 (s, 3H);

δC (100 MHz, $DMSO_4$-d_6) 165.52, 159.02, 156.66, 154.01, 153.84, 146.24, 130.40, 129.63, 127.62, 121.31, 114.19, 110.81, 110.34, 106.11, 18.30.

3.2.3.5. (E)-7-hydroxy-4-methyl-8-(((3-methylpyridin-2-yl)imino)methyl)-2H-chromen-2-one (3e)

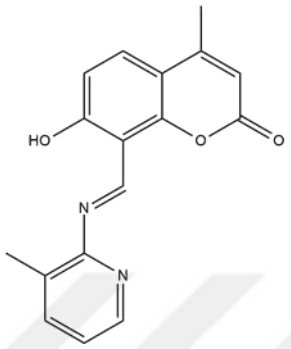

3e

Red crystal, yield: 66%

M.W.: 294.30 g/mol

Melting point: 230-231 ºC.

IR υmax (cm^{-1}): 3079 (O-H), 2982 (C-H), 1713 (C=O), 1625 (C=N), 1601 & 1556 (C=C), 1151 (C-N), 1072 (C-O)

δH (400 MHz, $DMSO_4$-d_6) 15.17 (s, 1H), 9.77 (s, 1H), 8.34 (d, J=8.8 Hz, 1H), 7.79-7.67 (m, 2H), 7.27 (d, J=8.8 Hz, 1H), 6.88 (t, J= 8.4 Hz, 1H), 6.13 (s, 1H), 2.52 (s, 3H), 2.32 (s, 3H);

δC (100 MHz, $DMSO_4$-d_6) 167.43, 163.73, 159.01, 156.06, 154.66, 146.53, 140.10, 131.28, 127.47, 123.49, 114.77, 112.36, 110.26, 105.99, 18.30, 16.66

3.2.4. General procedure of coumarin-hydrazone hybrids synthesis

2 and substituted hydrazine were added with ethanol as solvent into a flask, stirred for 3-6 h at room temperature (Fig.3.4). The reaction was monitored by thin layer chromatography TLC in 2:1 ethyl acetate/hexane, then filtered and washed out 3 times with ethanol. Solid product is obtained.

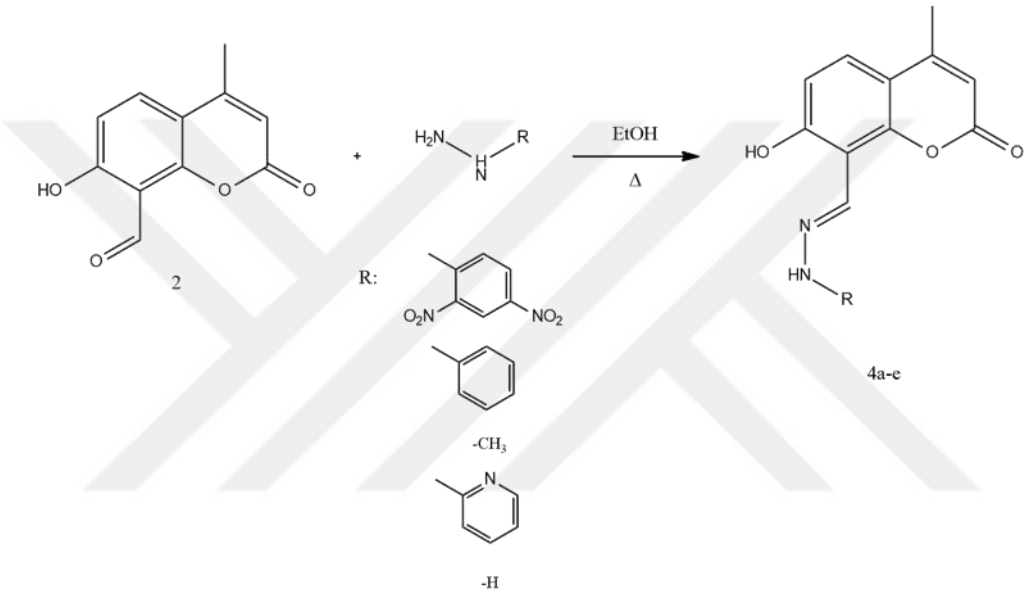

Figure 3.4. General synthesis reaction of coumarin-hydrazone hybrids

3.2.4.1. (E)-8-((2-(2,4-dinitrophenyl)hydrazono)methyl)-7-hydroxy-4-methyl-2H-chromen-2-one (4a)

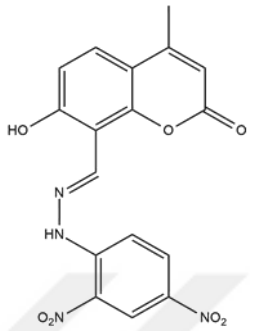

4a

Red crystal, yield: 59%

M.W.: 384.30 g/mol

Melting point: decomposed at 223 ºC.

IR υmax (cm^{-1}): 3281 (O-H), 3228 (N-H), 3089 (C-H), 1737 (C=O), 1655 (C=N), 1613 & 1586 (C=C), 1503 & 1325 (NO_2), 1139 (C-N), 1169 (N-N), 1069 (C-O)

δH (400 MHz, $DMSO_4$-d_6) 11.84 (s, 1H), 11.14 (s, 1H), 10.04 (s, 1H), 9.18 (s, 1H), 8.72 (d, J=8.8 Hz, 1H), 8.27 (d, J= 8.8 Hz, 1H), 7.66 (d, J=8.8 Hz, 1H), 6.87 (d, J= 8.8 Hz, 1H), 6.19 (s, 1H), 2.51 (s, 3H);

δC (100 MHz, $DMSO_4$-d_6) 166.50, 163.71, 158.91, 151.61, 148.55, 145.83, 145.75, 139.72, 130.32, 125.68, 124.76, 119.95, 117.31, 113.23, 112.53, 109.16 18.78.

3.2.4.2. (E)-7-hydroxy-4-methyl-8-((2-phenylhydrazono)methyl)-2H-chromen-2-one (4b)

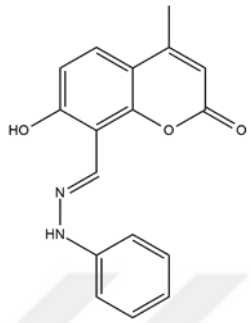

4b

Yellow crystal, yield: 68%

M.W.: 294.30 g/mol

Melting point: > 250 °C.

IR υmax (cm^{-1}): 3266 (O-H), 3133 (N-H), 3062 (C-H), 1705 (C=O), 1630 (C=N), 1598 & 1586 (C=C), 1181 (C-N), 1075 (C-O)

δH (400 MHz, $DMSO_4$-d_6) 12.08 (s, 1H), 10.89 (s, 1H), 8.62 (s, 1H), 7.65 (d, J=8.8 Hz, 1H), 7.35 (d, J=8.8 Hz, 2H), 6.96-6.80 (m, 4H), 6.26 (s, 1H), 2.54 (s, 3H);

δC (100 MHz, $DMSO_4$-d_6) 159.43, 159.35, 153.80, 151.22, 143.66, 133.66, 129.50, 125.83, 119.91, 112.90, 112.07, 111.79, 110.70, 106.73 18.29.

3.2.4.3. (E)-7-hydroxy-4-methyl-8-((2-methylhydrazono)methyl)-2H-chromen-2-one (4c)

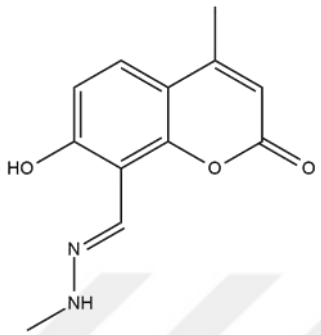

4c

Orange color crystal, yield: 65%

M.W.: 232.24 g/mol

Melting point: 166-168 ºC.

IR υmax (cm-1): 3349 (O-H), 3093 (N-H), 2879 (C-H), 1693 (C=O), 1656 (C=N), 1604 & 1577 (C=C), 1290 (C-N), 1164 (N-N), 1066 (C-O)

δH (400 MHz, $DMSO_4$-d_6) 12.70 (s, 1H), 10.41 (s, 1H), 7.94 (s, 1H), 7.49 (d, J=8.8 Hz, 1H), 6.83 (d, J=8.8 Hz, 1H), 6.17 (s, 1H), 2.91 (s, 3H), 2.37 (s, 3H);

δC (100 MHz, $DMSO_4$-d_6) 159.68, 159.52, 153.82, 150.63, 133.25, 128.09, 124.61, 112.84, 110.32, 107.19, 33.02, 18.25.

3.2.4.4. (E)-7-hydroxy-4-methyl-8-((2-(pyridin-2-yl)hydrazono)methyl)-2H-chromen-2-one (4d)

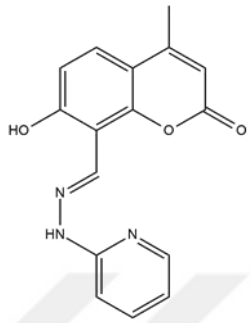

4d

Brown crystal, yield: 55%

M.W.: 295.29 g/mol

Melting point: decomposed at 156 ºC

IR υmax (cm-1): 3290 (O-H), 3204 (N-H), 2988 (C-H), 1734 (C=O), 1630 (C=N), 1595 & 1571 (C=C), 1228 (N-N), 1169 (C-N), 1069 (C-O)

δH (400 MHz, $DMSO_4$-d_6) 12.29 (s, 1H), 11.35 (s, 1H), 8.64 (s, 1H), 8.21 (d, J=8.8 Hz, 1H), 7.71-7.67 (m, 1H), 7.55 (d, J=8.8 Hz, 1H), 6.89-6.82 (m, 3H), 6.17 (s, 1H), 2.35 (s, 3H);

δC (100 MHz, $DMSO_4$-d_6) 159.86, 159.29, 154.78, 153.62, 151.47, 148.05, 138.21, 135.44, 126.12, 115.76, 113.02, 111.82, 110.57, 106.47, 106.42, 18.23.

3.2.4.5. 8,8'-((1E,1'E)-hydrazine-1,2-diylidenebis(methanylylidene))bis(7-hydroxy-4-methyl-2H-chromen-2-one) (4e)

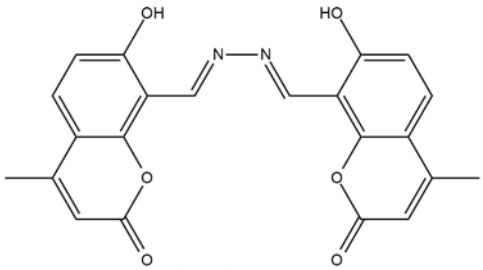

4e

Yellow crystal, yield: 41%

M.W.: 404.37 g/mol

Melting point: > 250 ºC.

IR υmax (cm-1): 3393 (O-H), 3958 (C-H), 1722 (C=O), 1622 (C=N), 1609 & 1574 (C=C), 1163 (N-N), 1072 (C-O)

δH (400 MHz, $CDCl_3$) 12.31 (s, 2H), 9.45 (s, 2H), 7.73 (d, J=9.2 Hz, 1H), 7.64 (d, J=8.8 Hz, 1H), 7.01 (d, J=8.8 Hz, 1H), 6.91 (d, J=8.8 Hz, 1H), 6.19 (s, 2H), 2.44 (s, 6H);

δC (100 MHz, $CDCl_3$) 159.95, 159.74, 154.18, 153.03, 147.70, 129.47, 114.29, 114.22, 112.10, 111.59, 18.89.

3.2.5. UV Absorbance and Fluorescence Emission Examination

Stock solutions were prepared at a fixed concentration 10 μM in 10 mL for each sample in 3 different solvents: Dimethyl sulfoxide (DMSO), Ethanol (EtOH) and Acetonitrile (ACN).

4. RESULTS AND DISCUSSION

Coumarin and its derivatives, commonly found in plants, are containing an α-pyrone ring fused with a benzene ring and used in several fields such as food, dye, perfume and drug industries. Coumarins are known of possessing fluorescence activities.

Schiff base on the other hand is an important class of compounds in organic and inorganic chemistry, is utilized in different industries. For instance; in medicine as a result of the pharmacological activity, as ligands or chemosensors in inorganic chemistry due to the ability to bind with metal ions.

Coumarin-imine or coumarin-hydrazone based Schiff bases have been produced for decades on different types of coumarins, amines and hydrazines. According to the literature, coumarin-imine and coumarin-hydrazone hybrids syntheses are usually performed in organic solvents media. Schiff base forms as a result of the condensation of formyl group on coumarin and the primary amine on aniline and hydrazine. General reaction and proposed mechanism shown below in (Fig.4.1 and 4.2).

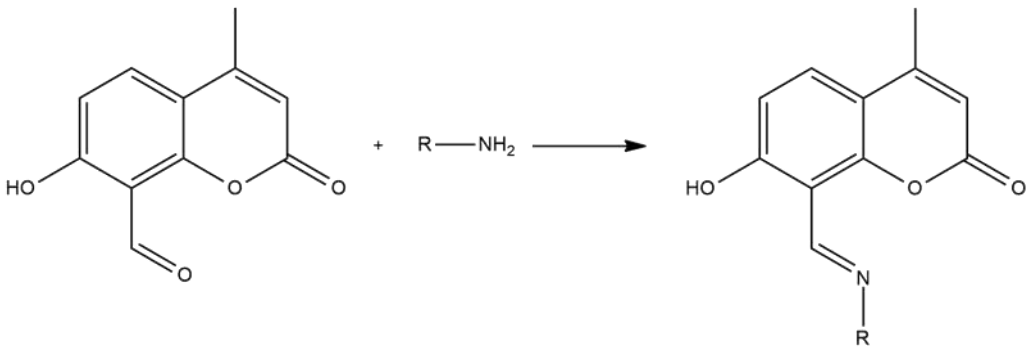

Figure 4.1. General reaction of coumarin derivatives synthesis

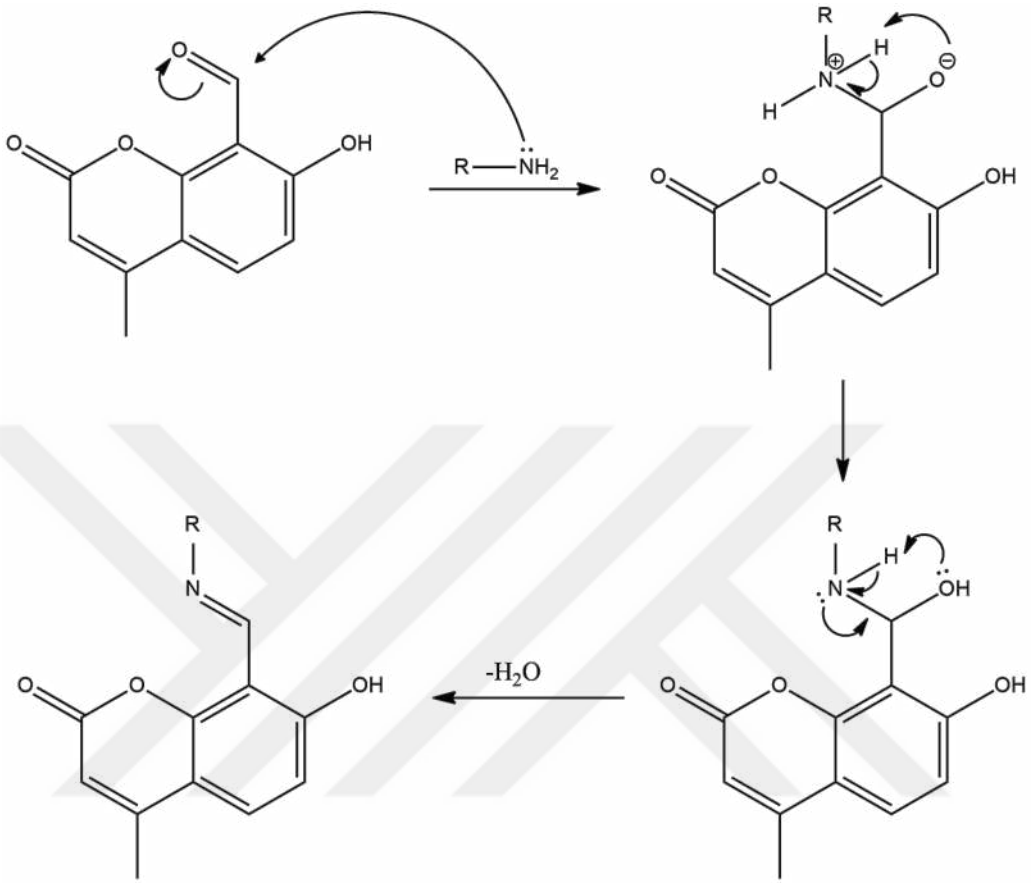

Figure 4.2. Proposed reaction mechanism of coumarin derivative formation

4.1. Coumarin-imine Hybrids Synthesis

Coumarin-imine (Schiff bases) were synthesized by the condensation of formyl group on compound **2** with primary amines in the presence of ethanol as a solvent and the absence of catalysts, refluxed for different durations as shown in Table 4.1.

Table 4.1. Different amines used to form Schiff base and reaction yields

Entry	Amine	Product	Time (h)	Yield (%)
2	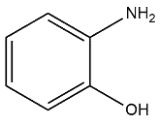 2-aminophenol	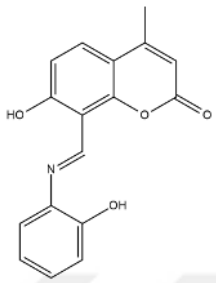 **3a**	6	90
2	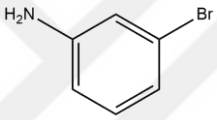 3-bromoaniline	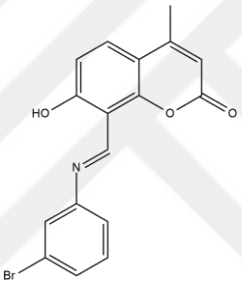 **3b**	3	87
2	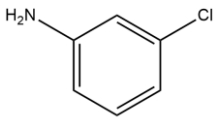 3-chloroaniline	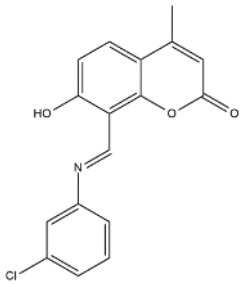 **3c**	3	78

2	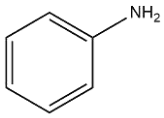 aniline	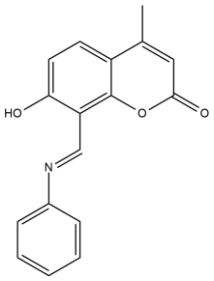 **3d**	3	67
2	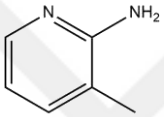 2-amine-3-methylpyridine	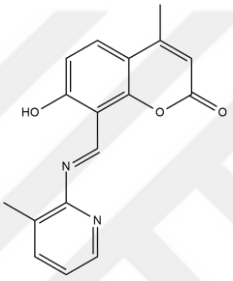 **3e**	3	66

According to data in (table.4.3), anilines possessing electron-donating substituent gave higher yield 90, 87 and 78% in **3a**, **3b** and **3c** respectively. Whereas in the case of **3d**, there was no substituent on aniline and the reaction yield was relatively lower 67%, and for 3e, -CH_3 is a weak electron-donating group and the reaction yield was only 66%.

4.2. Coumarin-hydrazone Hybrids Synthesis

Coumarin-hydrazone hybrids were synthesized by the condensation of formyl group on compound **2** with variety of hyrazines, in the presence of ethanol as a solvent, stirred at room temperature for different reaction time as shown in Table 4.2.

Table 4.2. Different substituted hydrazines used and reaction yields

Entry	Hydrazine	Product	Time (h)	Yield (%)
2	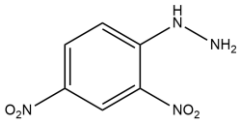 (2,4-dinitrophenyl)hydrazine	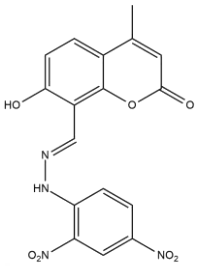 **4a**	3	58
2	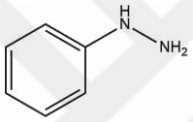 Phenylhydrazine	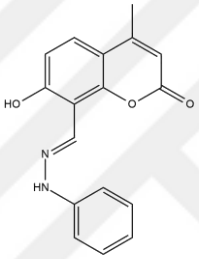 **4b**	6	68
2	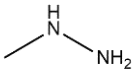 Methylhydrazine	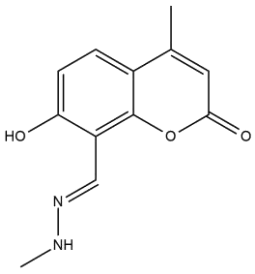 **4c**	6	64

2	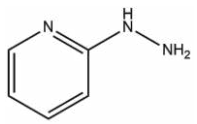 2-hydrazinopyridine	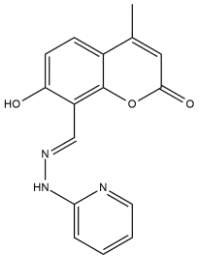 4d	6	55
2	$H_2N—NH_2$ Hydrazine	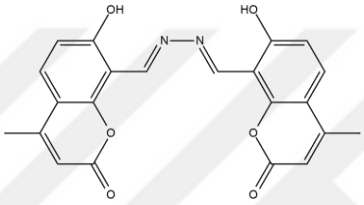 4e	24	40

4.3. UV-vis Absorbance and Fluorescence Activity

When a molecule was excited by the exposure to UV-vis light, electrons travel from electronic ground state to excited state. Fluorescence occurs when electrons travel from singlet excited state to the ground state emitting light in a certain frequency. Stokes shift is the difference between absorption and emission wavelengths and is simply calculated by the substraction of absorption wavelength from emission wavelength. The formula shown below:

$$\Delta\lambda = \lambda_{Em}\,\text{max} - \lambda_{Ex}\,\text{max}$$

Table 4.3. Fluorescence activity of the coumarin-imine and coumarin-hydrazone derivatives and Stokes shifts

	DMSO			EtOH			ACN		
	λ_{Em} (nm)	λ_{abs} (nm)	$\Delta\lambda$ (nm)	λ_{Em} (nm)	λ_{abs} (nm)	$\Delta\lambda$ (nm)	λ_{Em} (nm)	λ_{abs} (nm)	$\Delta\lambda$ (nm)
3a	472	348	124	340	230	110	338	208	130
3b	468	348	120	338	228	110	364	292	72
3c	472	346	126	340	230	110	370	292	78
3d	478	346	132	336	236	100	362	298	64
3e	456	346	110	354	232	122	366	300	66
4a	416	330	86	354	232	122	364	298	66
4b	438	348	90	338	228	110	368	292	76
4c	440	348	90	338	230	108	364	298	66
4d	456	342	114	446	232	214	370	294	76
4e	436	350	86	340	228	112	366	294	72

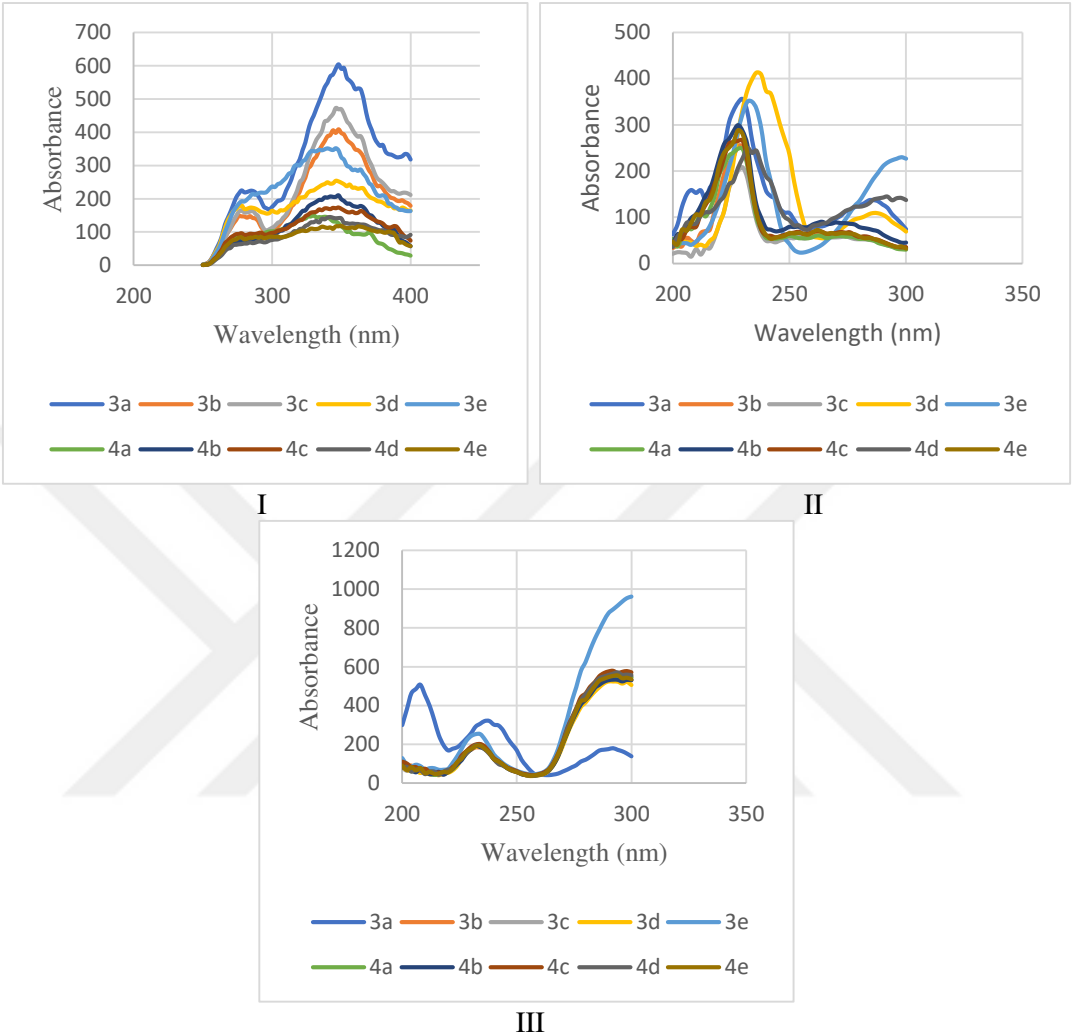

Figure 4.3. UV-vis absorption of fluorophores in: I. DMSO, II. EtOH, III. ACN

Considering data in Table 4.3 and Fig.4.3, all fluorophores showed UV-vis absorption maxima at relatively similar wavelength in each of the three solvents. In DMSO, absorption maxima were between 330 – 350 nm, 228 – 236 nm in ethanol and 292 – 300 in ACN except for 3a which showed absorption maximum at 208 nm (Fig.4.3).

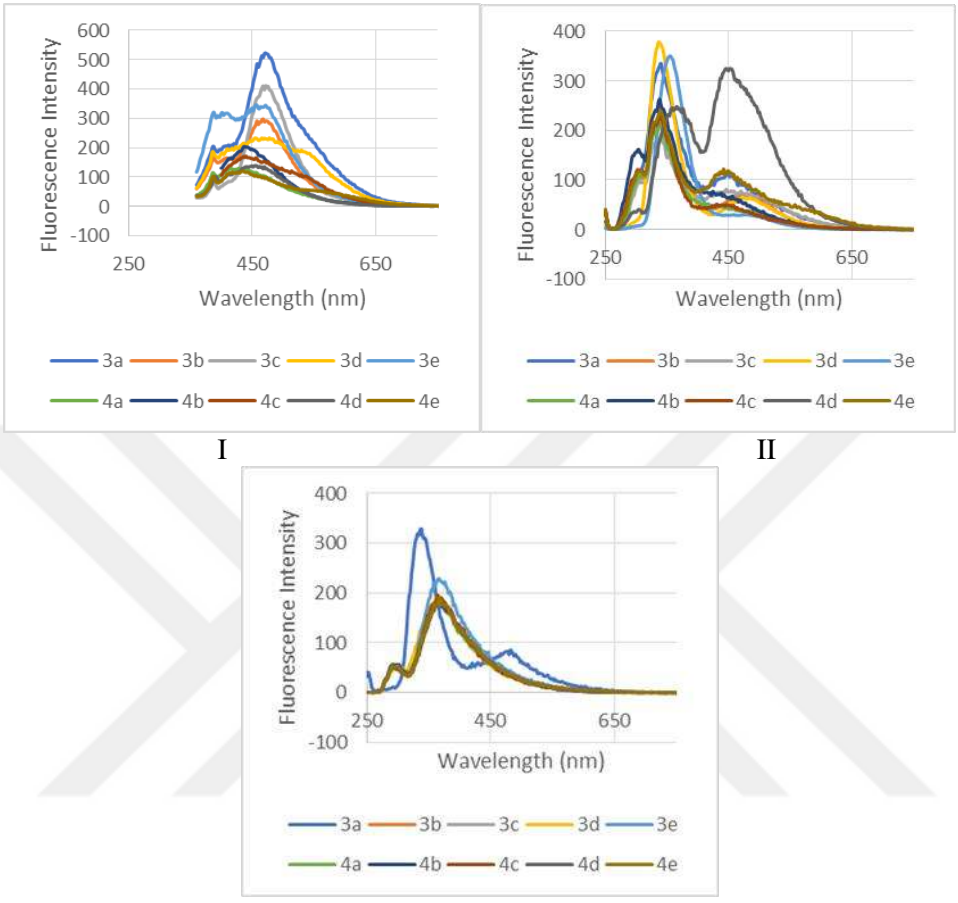

Figure 4.4. Fluorescence spectra in: I. DMSO, II. EtOH, III. ACN

According to values given in Table 4.3 and Fig 4.4, emission maxima and spectral shape of fluorophores vary from a solvent to the other. Maximum values in DMSO were red-shifted and fell between 438 – 472 nm except for 4a which was at 416 nm, while in ethanol the range was between 336 – 354 nm except 4d which was at 452 which in turn exhibited the largest Stokes shift among all the fluorophores - according to the literature, above 80 nm, is recognized as large Stokes shift-(Gao et al., 2017), and finally in ACN, the fluorophores exhibited fluorescence between 364 – 370 nm, excluding 3a which showed at 338 nm. Stokes shift lengths varied depending on the solvent. All fluorophores had Stokes shifts above 100 nm which

can be considered as molecules with large Stokes shift. Largs Stokes shift is essential in the applications of bioimaging. It minimizes spectral overlapping of absorption and emission on each other and prevents self-quenching, consequently, it enhances the ability to differentiate between the light coming from the excitation source and the emitted light (Gao et al., 2017). Coumarin-hydrazone derivatives **4a**, **4b**, **4c** and **4e** exhibited significant decline in Stokes shift values compared to coumarin-imine derivatives in DMSO, in the range between 86 nm and 92 nm which is still above 80 nm and can be considered as large Stokes shift.

3a in DMSO absorbed at 348 nm and 472 nm in the visible range. Absorption and emission maxima were red-shifted and more intense comparing with EtOH and ACN, which absorbed at 230 nm and emitted at 340 nm in EtOH, and absorbed at 208 nm and emitted at 338 nm in ACN. **3a** exhibited largest Stokes shift in ACN with a difference of 130 nm between absorption and emission maxima, then a smaller 124 nm in DMSO and 110 nm in EtOH (Table 4.3) (Fig.4.5).

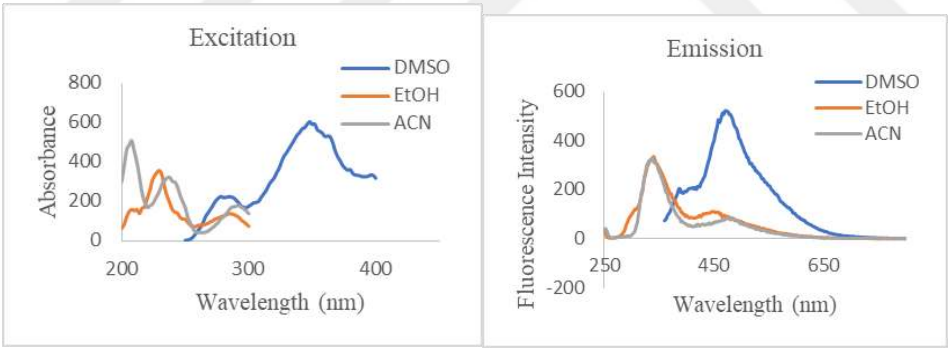

Figure 4.5. Excitation and emission wavelength diagram of 3a

According to data given in table 4.3 and (Fig.4.6), **3b** in DMSO absorbed UV-vis at 348 nm and fluoresced at 468 nm in the visible range, while it absorbed at 228 nm in EtOH and 292 nm in ACN, and fluoresced at 338 in EtOH and 364 in ACN. Stokes shifts were calculated as 120 nm, 110 nm and 72 nm in DMSO, EtOH and ACN respectively.

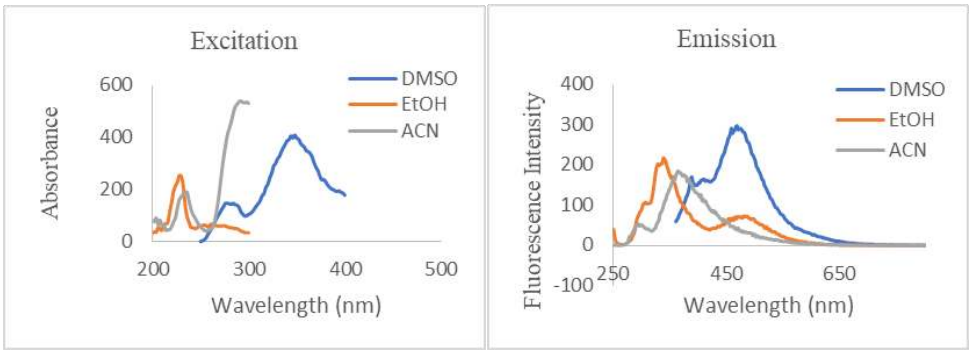

Figure 4.6. Excitation and emission wavelength diagram of 3b

Calculations based on data in table 4.3, showed 125 nm as Stokes shift of **3c** in DMSO, 110 nm in EtOH and 78 nm in ACN. **3c** exhibited absorption at 346 nm and emission at 472 nm in DMSO, absorption at 230 nm and emission at 340 nm in EtOH, and absorption at 292 nm and emission at 370 nm in ACN (Fig.4.7).

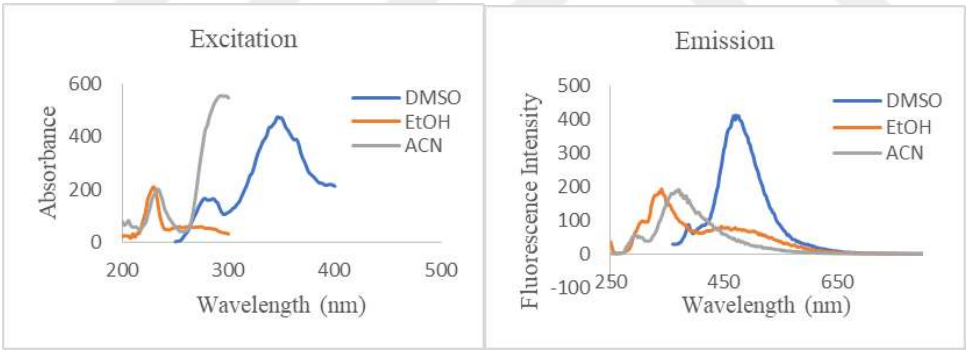

Figure 4.7. Excitation and emission wavelength diagram of 3c

3d exhibited the largest Stokes shift among other fluorophores of this study in DMSO with a distance of 132 nm between absorption maximum at 346 nm and fluorescence maximum at 478 nm, while in EtOH, 3d absorbed at 234 nm and emitted at 336 nm with 100 nm of Stokes shift, and in ACN, it absorbed at 298 nm and emitted at 362 nm showing 64 nm as Stokes shift representing the smallest

Stokes shift among all the fluorophores in this study (Fig.4.8). Besides, **3d** showed relatively steady intensity of fluorescence between 338 nm and 548 nm.

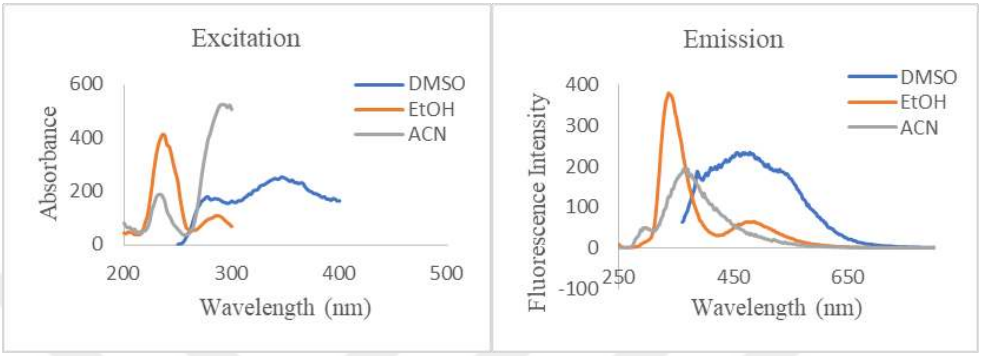

Figure 4.8. Excitation and emission Wavelength diagram of 3d

3e's absorption and emission maxima were located at 346 nm and 456 nm in DMSO respectively, manifesting 110 nm Stokes shift, where in EtOH, it exhibited absorption at 232 nm and emission at 354 nm with 122 nm as Stokes shift, and it absorbed at 300 nm and emitted at 366 nm making the difference between absorption and emission equals 66 nm (Fig.4.9). Besides relative steadiness in the fluorescence intensity between 393 nm and 478 nm.

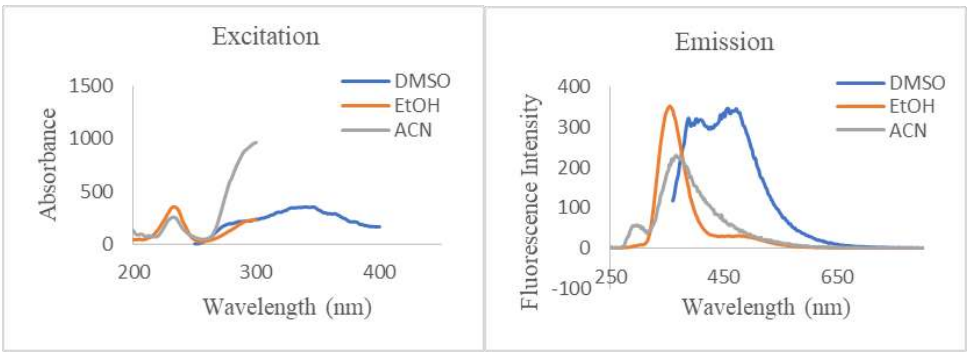

Figure 4.9. Excitation and emission wavelength diagram of 3e

4a in DMSO absorbed UV-vis at 330 nm and emitted at 416 nm resulting 86 nm as Stokes shift. 4a in EtOH absorbed at 228 nm and emitted at 338 nm with Stokes shift gap of 110 nm, and in ACN, it absorbed at 298 nm and emitted at 364 nm leaving 66 nm as Stokes shift (Fig.4.10).

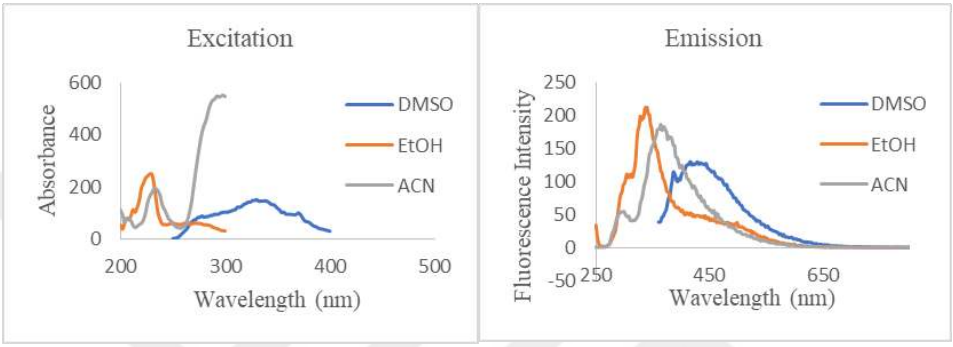

Figure 4.10. Excitation and emission wavelength diagram of 4a

The compound **4b** absorbed at 348 nm and emitted at 438 nm in DMSO, absorbed at 228 nm and emitted at 338 nm in EtOH and absorbed at 292 nm and emitted at 368 nm in ACN. The Stokes shifts were 90,110 and 76 nm in DMSO, EtOH and ACN respectively (Fig 4.11).

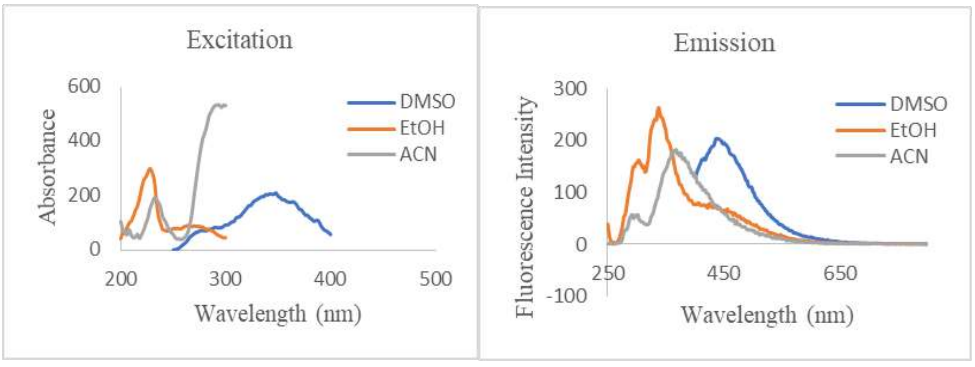

Figure 4.11. Excitation and emission wavelength diagram of 4b

4c exhibited absorption at 348 nm and emission at 440 nm in DMSO, absorption at 230 nm and emission at 338 nm in EtOH and absorption at 298 nm and emission at 364 nm. The Stokes shifts were 92, 108 and 66 nm in DMSO, EtOH and ACN respectively (Fig.4.12).

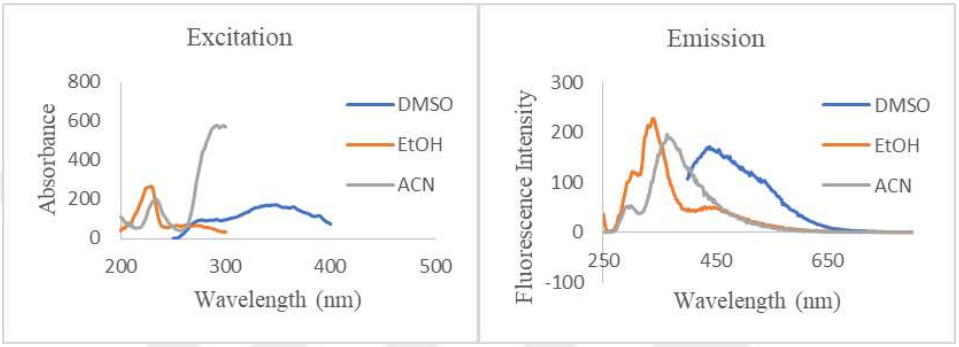

Figure 4.12. Excitation and emission wavelength diagram of 4c

4d in DMSO, showed maximum absorption at 342 nm and maximum emission at 456, absorption at 232 nm and emission at 446 nm in EtOH in the visible range and absorption at 294 nm and emission at 370 nm in ACN. According to calculations, Stokes shifts were 114, 214 and 76 nm in DMSO, EtOH and ACN respectively (Fig.4.13). Stokes shift occurred in EtOH was interesting, it was the largest among all the samples, **4d** in EtOH exhibited 2 substantial bands of emission with high intensity as shown in (Fig.4.13).

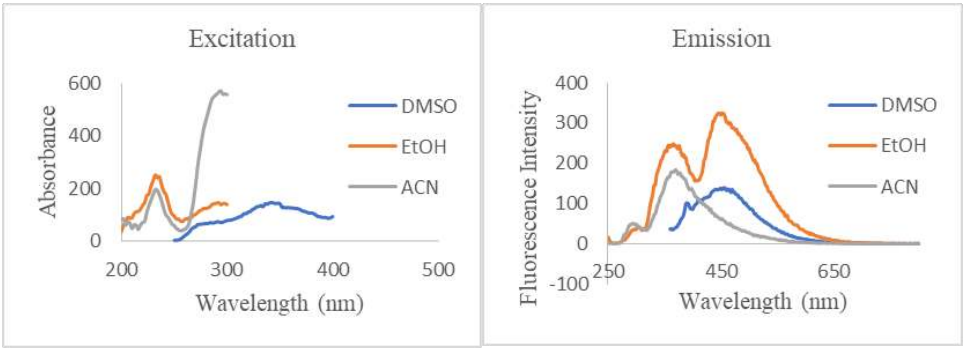

Figure 4.13. Excitation and emission wavelength diagram of 4d

Finally, **4e** showed absorption at 350 nm and emission at 436 nm in DMSO, absorption at 228 nm and emission at 340 nm in EtOH and absorption at 294 nm and emission at 336 nm in ACN. Stokes shifts for **4e** were 86, 112 and 72 nm in DMSO, EtOH and ACN respectively (Fig.4.14).

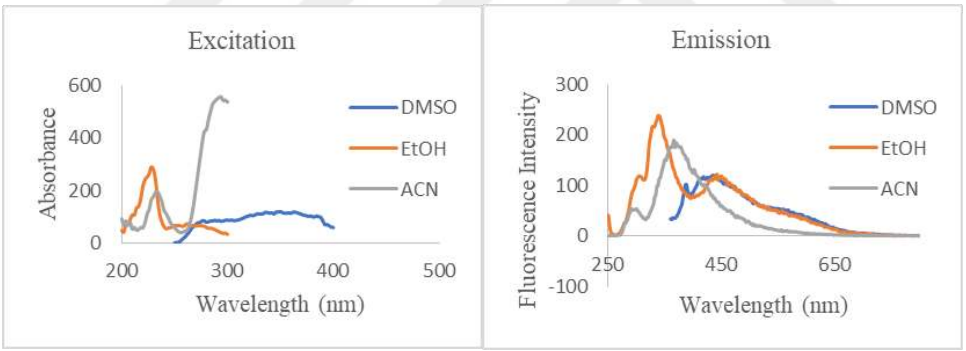

Figure 4.14. Excitation and emission wavelength diagram of 4e

Fluorophores in ACN and **3e** in DMSO, show minor band besides the maximum. However, **3d** in ethanol shows significantly intense minor band at 366 nm. It had been known that coumarin based fluorophores don't usually show dual emission band. This type of fluorophores can be used as bioimaging fluorescent (Huang et al., 2010; Xie et al., 2012).

It was observed that all fluorophores showed high absorbance intensity at their absorption maxima in ACN, yet, they had smaller Stokes shifts except for **3a**,

it didn’t show high absorption intensity, nevertheless, it had considerably large Stokes shift.

5. CONCLUSION

Literature has numerous studies on coumarin, Schiff base and their derivative and hybrid synthesis. These coumarin derivatives have won their position in the industry fields due to the biological and pharmacological activities. Thus, many methods have been developed for coumarin synthesis and derivation.

In this study, ten novel coumarin derivatives were designed and synthesized. Coumarin was produced through Pechmann Reaction, then C-8 of the coumarin was formylated, then as final stage Schiff bases – imines and hydrazones - were formed by the condensation of the formyl group on the coumarin with a variety of primary amines and hydrazines. Chemical structure of each product was confirmed via IR and ^{1}H NMR and ^{13}C NMR.

Fluorescence activity was investigated in three different solvents: DMSO, ethanol and acetonitrile. Absorption and emission maxima were brought to light. Stokes shifts were calculated. Generally, all ten fluorophores had large Stokes shifts in DMSO and EtOH, however, it wasn't the case in ACN.

For future studies, Schiff bases can be formed and investigated on different carbon on the skeleton of coumarin using the same amines. Comparison can be done on some group of molecules other than primary amines, attached to C-8 on coumarin. For fluorophores produced in this study, fluorescence activity can be investigated in various set of solvents, different temperatures, concentrations, polarities and acidities.

Since Schiff bases possess lone electron-pairs and have high sensitivity and the ability to function as a ligand and form coordination bonds with metals, it is suggested additional studies to be done on the fluorophores in this study, in order to measure the impact of the metals on the fluorescence activities and seek suitable applicable fields.

REFERENCES

Ashoor, L. S., Mohaisen, I. K., & Al-Shemary, R. K. R., 2020. A review on synthesis and versatile applications of some selected schiff bases with their transition metal complexes. *Egyptian Journal of Chemistry*, *63*(December), 523–547.

Bargellini, L., Forti-Forti., 1911 Gazz. Chim. Ital., 41 (I); 750.

Corrie, J. E. T., 1990. A convenient synthesis of N-(7-dimethylamino-4-methylcoumarin-3-yl)- maleimide incorporating a novel variant of the Pechmann reaction. *Journal of the Chemical Society, Perkin Transactions 1*, *7*, 2151–2152.

Eck, M., 2017. *Dissertation zur Erlangung des Doktorgrades der Technischen Fakultät der Albert-Ludwigs-Universität Freiburg im Breisgau Performance enhancement of hybrid nanocrystal / polymer bulk heterojunction solar cells : aspects of device efficiency , reproducibili*. *January 2014*.

Erşatır, M., Akbaşlar, D., Demirkol, O., Giray, E. S., 2016. Cross-Aldol reaction of 3-acetyl-2H-chromen-2-one by Using Amberlyst 26A as Catalyst, *Synthetic Communications*, 47:1, 68-77.

Forman, S. E., 1964. Synthesis of Oximes. *Journal of Organic Chemistry*, *29*(11), 3323–3327.

Fylaktakidou, K., Hadjipavlou-Litina, D., Litinas, K., & Nicolaides, D., 2005. Natural and Synthetic Coumarin Derivatives with Anti-Inflammatory / Antioxidant Activities. *Current Pharmaceutical Design*, *10*(30), 3813–3833.

Gao, Z., Hao, Y., Zheng, M., & Chen, Y., 2017. A fluorescent dye with large Stokes shift and high stability: synthesis and application to live cell imaging. *RSC Advances*, *7*(13), 7604–7609.

Harayama, T., Ishii, H., Kaneko, Y., & Miyazaki, H., 1991. NII-Electronic Library Service. *Chemical Pharmaceutical Bulletin*, *43*, 2091.

Heravi, M. M., Zadsirjan, V., Hamidi, H., Daraie, M., & Momeni, T., 2020. Recent applications of the Wittig reaction in alkaloid synthesis. In *Alkaloids: Chemistry and Biology* (1st ed., Vol. 84). Elsevier Inc.

Hoefnagel, A. J., Gunnewegh, E. A., Downing, R. S., & Van Bekkum, H., 1995. Synthesis of 7-hydroxycoumarins catalysed by solid acid catalysts. *Journal of the Chemical Society, Chemical Communications*, *105*(2), 225–226.

Hoesch, K., 1915 A New Synthesis of Aromatic Ketones. I. Preparation of Some Phenol Ketones. *Berichte der Deutschen Chemischen Gesellschaft*, 48; 1122-1133.

Huang, S. T., Jian, J. L., Peng, H. Z., Wang, K. L., Lin, C. M., Huang, C. H., & Yang, T. C. K., 2010. The synthesis and optical characterization of novel iminocoumarin derivatives. *Dyes and Pigments*, *86*(1), 6–14.

Hussien, F. A. H., Keshe, M., Alzobar, K., Merza, J., & Karam, A. (2016). Synthesis and Nitration of 7-Hydroxy-4-Methyl Coumarin via Pechmann Condensation Using Eco-Friendly Medias. *International Letters of Chemistry, Physics and Astronomy*, *69*, 66–73.

Jameson, D. M., Croney, J. C., & Moens, P. D. J. (2003). Fluorescence: Basic concepts, practical aspects, and some anecdotes. *Methods in Enzymology*, *360*, 1–43.

Kadnikov, D. V., & Larock, R. C. (2003). Palladium-catalyzed carbonylative annulation of terminal alkynes: Synthesis of coumarins and 2-quinolones. *Journal of Organometallic Chemistry*, *687*(2), 425–435.

Kim, W. Y., Shi, H., Jung, H. S., Cho, D., Verwilst, P., Lee, J. Y., & Kim, J. S. (2016). Coumarin-decorated Schiff base hydrolysis as an efficient driving force for the fluorescence detection of water in organic solvents. *Chemical Communications*, *52*(56), 8675–8678.

Kim, Y. H., Choi, M. G., Im, H. G., Ahn, S., Shim, I. W., & Chang, S. K. (2012). Chromogenic signalling of water content in organic solvents by hydrazone-acetate complexes. *Dyes and Pigments*, *92*(3), 1199–1203.

Knoevenagel, E. (1896). *The Knoevenagel Condensation*. *15*(04), 0428.

Kostanecki, V., & Rozycki, A. (1901). *Ueber eine Bildungsweise von Chromonderivaten.*

Kulkarni, A., Patil, S. A., & Badami, P. S. (2008). Synthesis, characterization, DNA cleavage and in vitro antimicrobial studies of La(III), Th(IV) and VO(IV) complexes with Schiff bases of coumarin derivatives. *European Journal of Medicinal Chemistry*, *44*(7), 2904–2912.

Kumar, V., Tomar, S., Patel, R., Yousaf, A., Parmar, V. S., & Malhotra, S. V. (2008). FeCl3-catalyzed Pechmann synthesis of coumarins in ionic liquids. *Synthetic Communications*, *38*(15), 2646–2654.

Lakowicz, J. R. (2000). *Instrumentation for Fluorescence Spectroscopy 2.1.* 27–61.

Lakowicz, J. R. (2006a). Chapter 1 Principles of Fluorescence. *Principles of Fluorescence Spectroscopy*, *32*(1), 1–26.

Lakowicz, J. R. (2006b). Chapter 24 - Fluorescence Correlation Spectroscopy. *Principles of Fluorescence Spectroscopy*, *74*(7), 797.

Lingaraju, G. S., Balaji, K. S., Jayarama, S., Anil, S. M., Kiran, K. R., & Sadashiva, M. P. (2018). Synthesis of new coumarin tethered isoxazolines as potential anticancer agents. *Bioorganic and Medicinal Chemistry Letters*, *28*(23–24), 3606–3612.

Mahapatra, A. K., Hazra, G., Roy, J., & Sahoo, P. (2011). A simple coumarin-based colorimetric and ratiometric chemosensor for acetate and a selective fluorescence turn-on probe for iodide. *Journal of Luminescence*, *131*(7), 1255–1259.

Matos, M. J., Viña, D., Vazquez-Rodriguez, S., Uriarte, E., & Santana, L. (2012). Send Orders of Reprints at reprints@benthamscience.net Focusing on New Monoamine Oxidase Inhibitors: Differently Substituted Coumarins As An Interesting Scaffold. *Current Topics in Medicinal Chemistry*, *12*, 2210–2239.

Munjanja, B., & Sanganyado, E. (2015). High-Performance Liquid

Chromatography: An Established Separation Technique in Food Chemistry. *Handbook of Food Analysis - Two Volume Set*, *December 2016*, 1301–1322.

Narasimhan, N. S., Mali, F. S., & Barve, M. V. (1979). *Synthetic Application of Lithian Reactions: Part XIII. Synthesis of 3-Phenylcoumarin and their Benzo Derivatives*.

Ngoc Toan, V., & Dinh Thanh, N. (2020). Synthesis of 6- and 7-alkoxy-4-methylcoumarins from corresponding hydroxy coumarins and their conversion into 6- and 7-alkoxy-4-formylcoumarin derivatives. *Synthetic Communications*, *50*(23), 3603–3615.

Novak, I., & Kovač, B. (2000). UV photoelectron spectroscopy of coumarins. *Journal of Electron Spectroscopy and Related Phenomena*, *113*(1), 9–13.

Öztürk, C. (2007). Determination of thyroxine hormone based on fluorescence quenching of 7-hydroxy coumarin. In *Hacettepe University* (Vol. 67, Issue 6).

Pérez-Cruz, K., Moncada-Basualto, M., Morales-Valenzuela, J., Barriga-González, G., Navarrete-Encina, P., Núñez-Vergara, L., Squella, J. A., & Olea-Azar, C. (2018). Synthesis and antioxidant study of new polyphenolic hybrid-coumarins. *Arabian Journal of Chemistry*, *11*(4), 525–537.

Schiff, H. (1869). Untersuchungen über Salicinderivate; *Justus Liebigs Annalen Der Chemie*, *150*(2), 193–200.

Sethna, S. M., Shah, N. M., & Shah, R. C. (1938). Aluminium chloride, a new reagent for the condensation of β-ketonic esters with phenols - Part I. The Condensation of Substituted Resacetophenones with Ethyl Acetoacetate. *Proceedings of the Indian Academy of Sciences - Section A*, *13*(5), 352–358.

Sethna, Suresk M., & Shah, N. M. (1945). The chemistry of coumarins. *Chemical Reviews*, *36*(1), 1–62.

Simpson, J. D., & Stephen, H. (1956). *The Reaction between Cinnamic Acid and Phenols in Presence of Hydrochloric Acid. A New Method for the Preparation of 3 : 4-Di- hydro-4 - phenylcoumarins. 1382*, 1382–1384.

Shiraishi, Y., Hayashi, N., Nakamura, M., & Hirai, T. (2016). Coumarin-imine-quinoxaline linkage designed based on the strecker reaction as a receptor for fluorometric cyanide anion detection in neutral media.

Shiraishi, Y., Yamada, C., & Hirai, T. (2019). A coumarin-dihydroperimidine dye as a fluorescent chemosensor for hypochlorite in 99% water. *RSC Advances*, *9*(49), 28636–28641.

Tapanyiğit, O., Demirkol, O., Güler, E., Erşatır, M., Çam, M. E., & Giray, E. S. (2020). Synthesis and investigation of anti-inflammatory and anticonvulsant activities of novel coumarin-diacylated hydrazide derivatives. *Arabian Journal of Chemistry*, *13*(12), 9105–9117.

Valeur, B., & Brochon, J.-C. (2001). New trends in fluorescence spectroscopy : applications to chemical and life science. In *Springer series on fluorescence*.

Von Pechmann, H., & Duisberg, C. (1883). Ueber die Verbindungen der Phenole mit Acetessigäther. *Berichte Der Deutschen Chemischen Gesellschaft*, *16*(2), 2119–2128.

Xie, L., Chen, Y., Wu, W., Guo, H., Zhao, J., & Yu, X. (2012). Fluorescent coumarin derivatives with large stokes shift, dual emission and solid state luminescent properties: An experimental and theoretical study. *Dyes and Pigments*, *92*(3), 1361–1369.

Zhuang, X., Liu, W., Wu, J., Zhang, H., & Wang, P. (2011). A novel fluoride ion colorimetric chemosensor based on coumarin. *Spectrochimica Acta - Part A: Molecular and Biomolecular Spectroscopy*, *79*(5), 1352–1355.

BACKGROUND

Makki Azzaman. He attended his elementary, intermediate and high schools in Makkah. He took an English Language course at National University of Modern Languages in Islamabad – Pakistan in 2010-2011. He graduated in the Department of Chemistry at Taif University in Taif City – Saudi Arabia in 2016. In 2017, he got the chance to pursue Master's Degree in Chemistry in the Republic of Turkiye. He speaks four languages fluently.

APPENDIX

Attachment 1. ^{1}H NMR spectrum of 7-hydroxy-4-methyl-2H-chromen-2-one

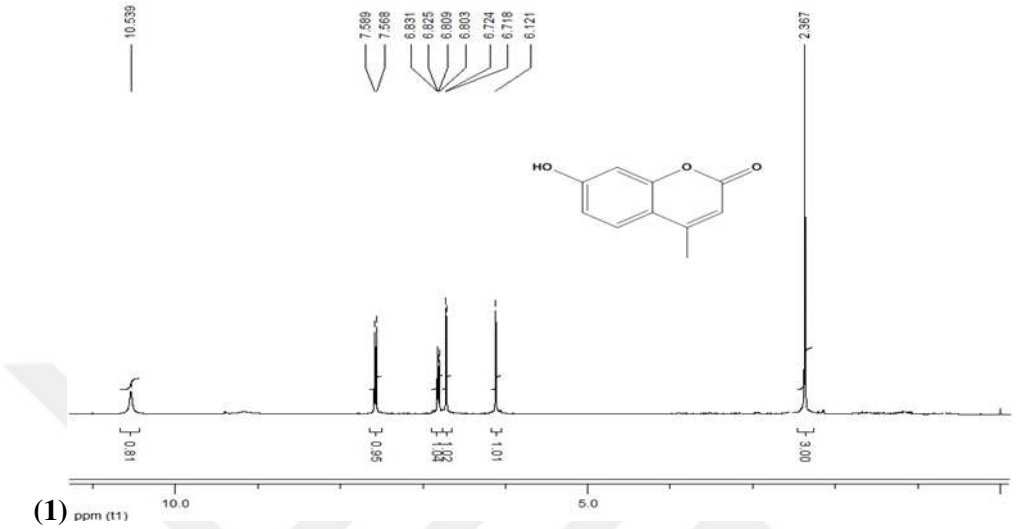

(1)

Attachment 2. ^{13}C NMR spectrum of 7-hydroxy-4-methyl-2H-chromen-2-one

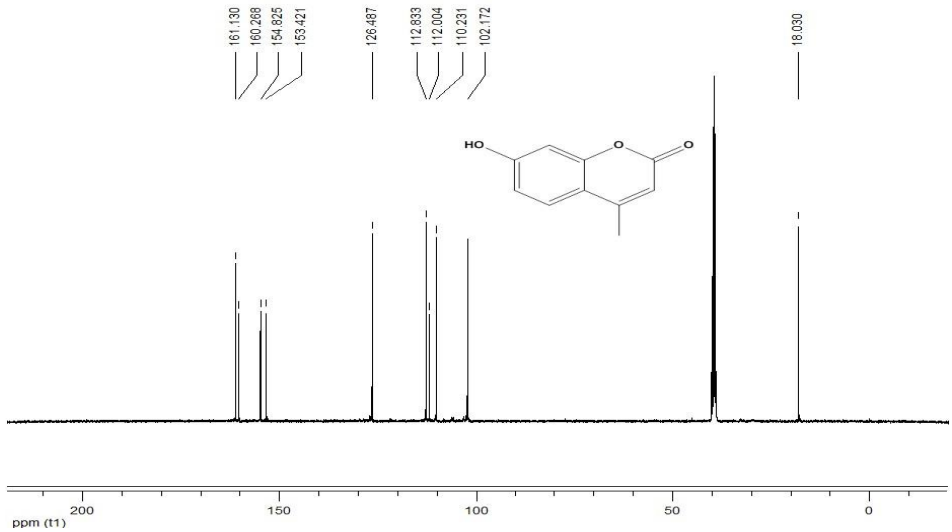

(1)

Attachment 3. FT-IR spectrum of 7-hydroxy-4-methyl-2H-chromen-2-one (1)

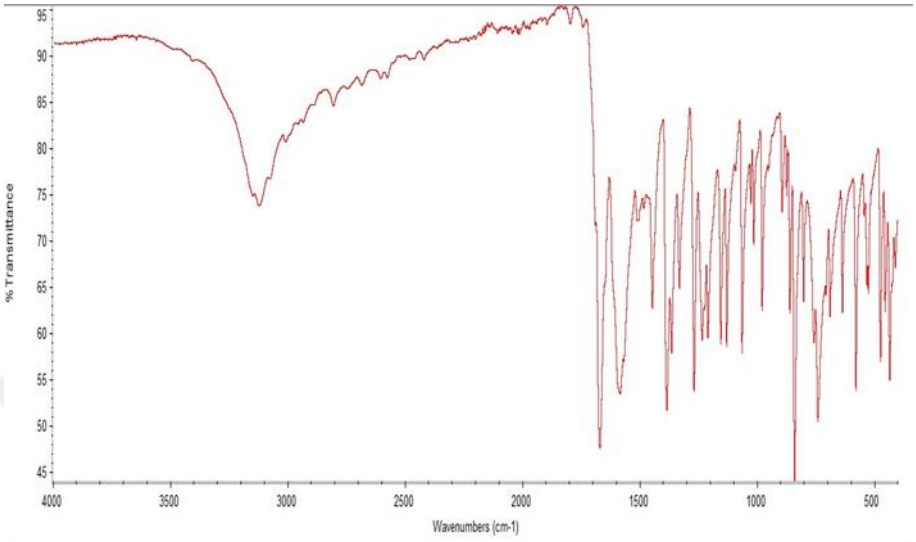

Attachment 4. ^{1}H NMR spectrum of 7-hydroxy-4-methyl-2-oxo-2H-chromene-8-carbaldehyde (2)

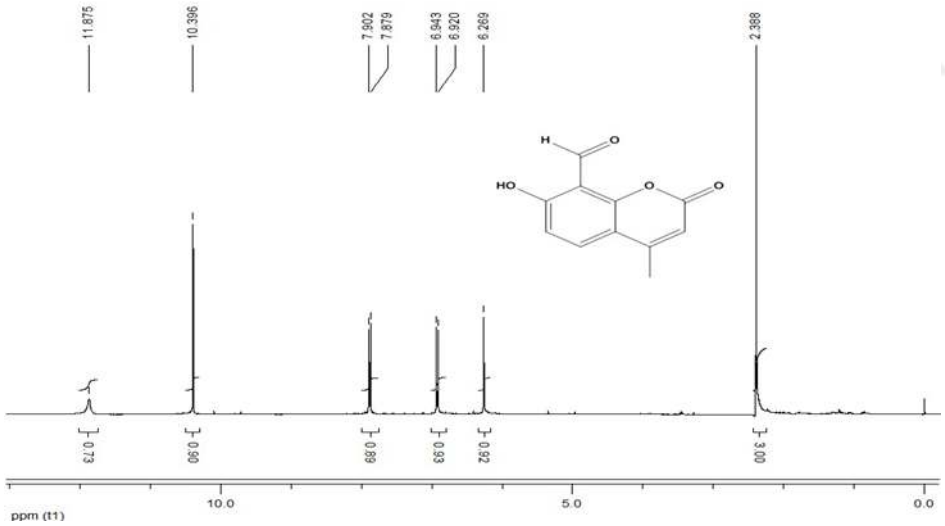

Attachment 5. ^{13}C NMR spectrum of 7-hydroxy-4-methyl-2-oxo-2H-chromene-8-carbaldehyde (2)

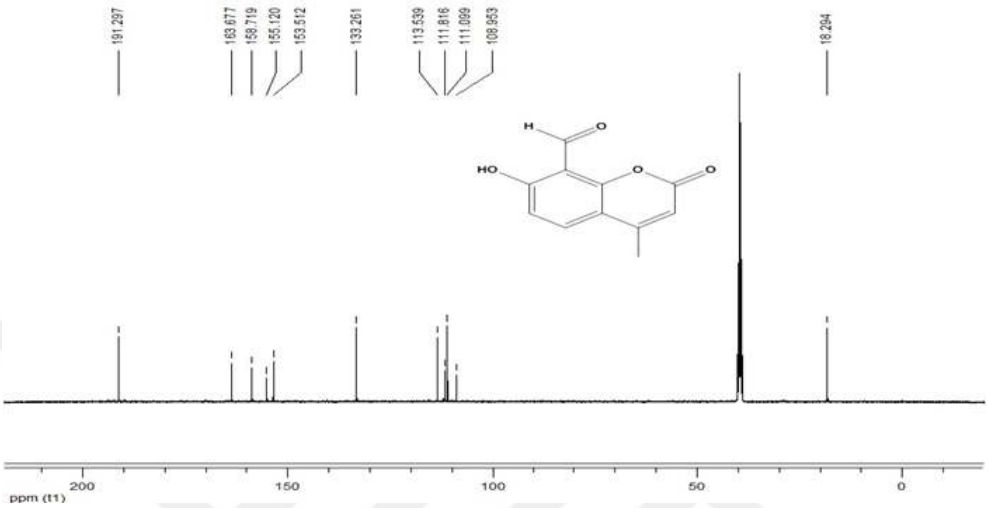

Attachment 6. FT-IR spectrum of 7-hydroxy-4-methyl-2-oxo-2H-chromene-8-carbaldehyde (2)

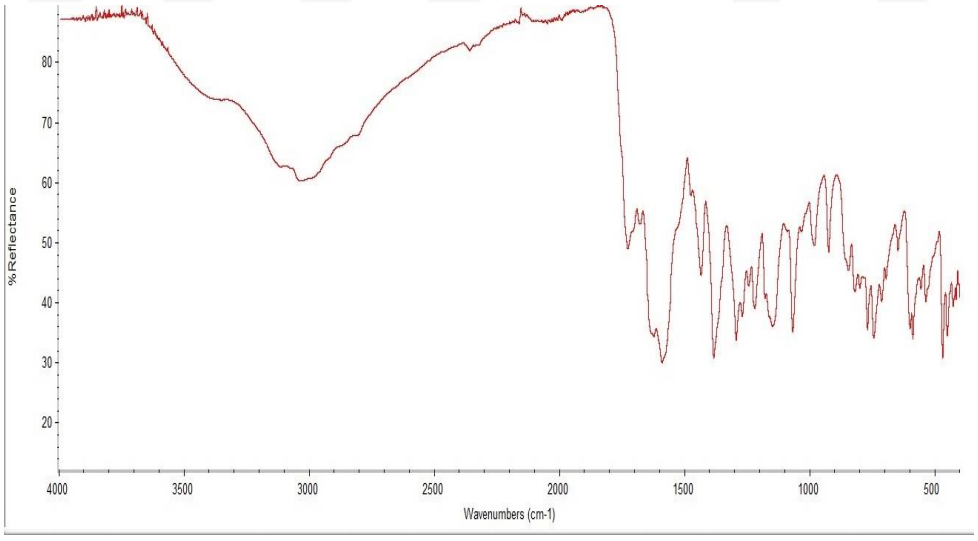

Attachment 7. ^{1}H NMR spectrum of (E)-7-hydroxy-8-(((2-hydroxyphenyl)imino)methyl)-4-methyl-2H-chromen-2-one (3a)

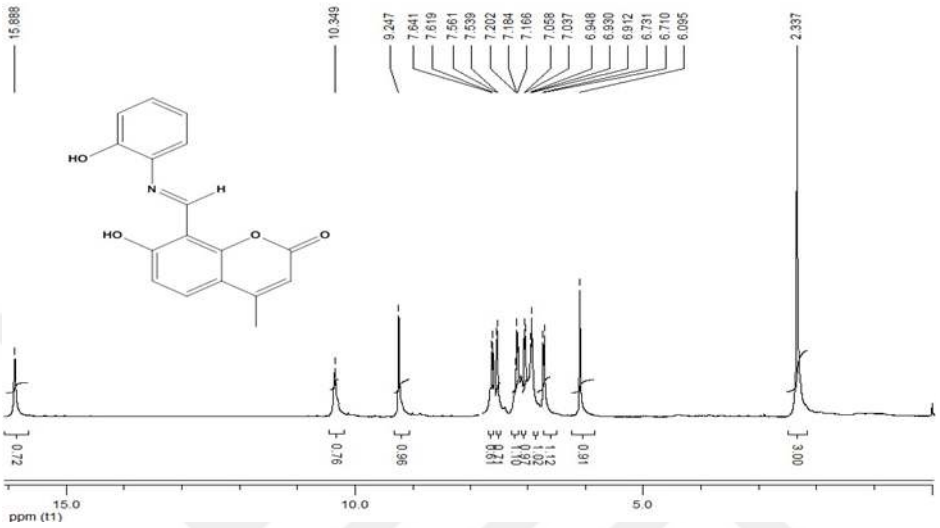

Attachment 8. ^{13}C NMR spectrum of (E)-7-hydroxy-8-(((2-hydroxyphenyl)imino)methyl)-4-methyl-2H-chromen-2-one (3a)

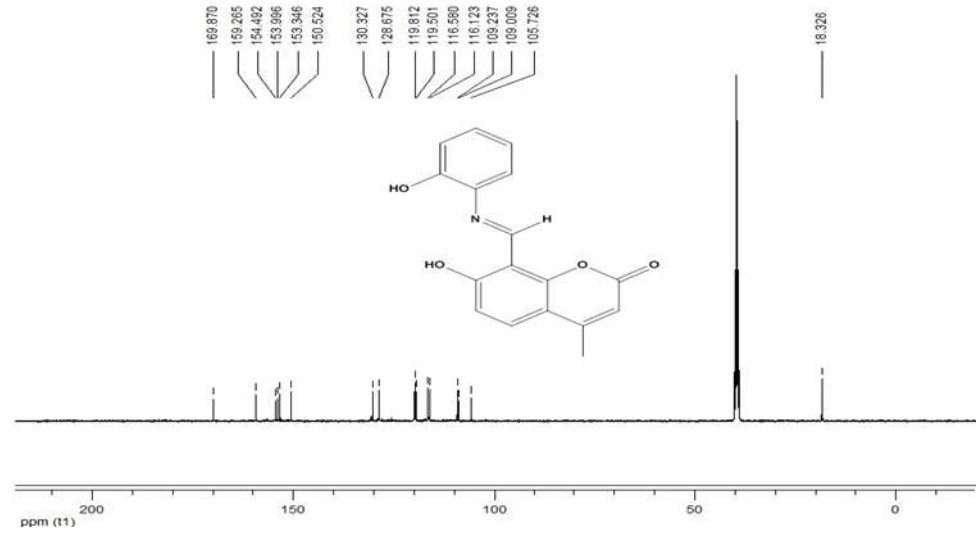

Attachment 9. FT-IR spectrum of (E)-7-hydroxy-8-(((2-hydroxyphenyl) imino)methyl)-4-methyl-2H-chromen-2-one (3a)

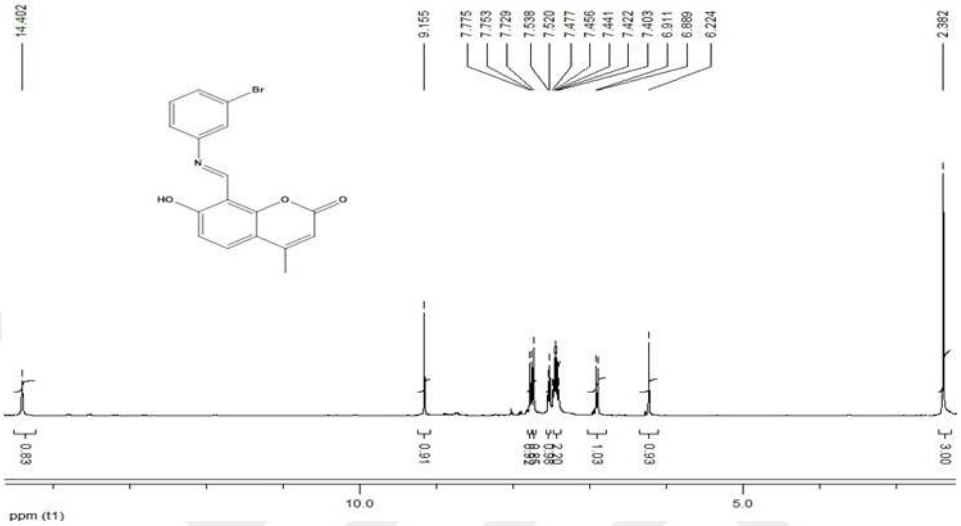

Attachment 10. ^{1}H NMR spectrum of (E)-8-(((3-bromophenyl)imino)methyl)-7-hydroxy-4-methyl-2H-chromen-2-one (3b)

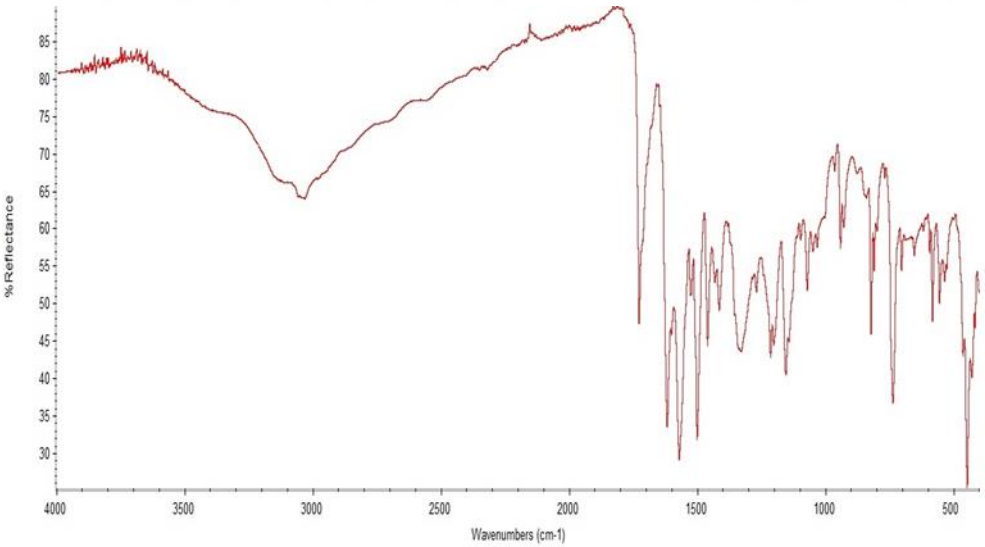

Attachment 11. ^{13}C NMR spectrum of (E)-8-(((3-bromophenyl)imino)methyl)-7-hydroxy-4-methyl-2H-chromen-2-one (3b)

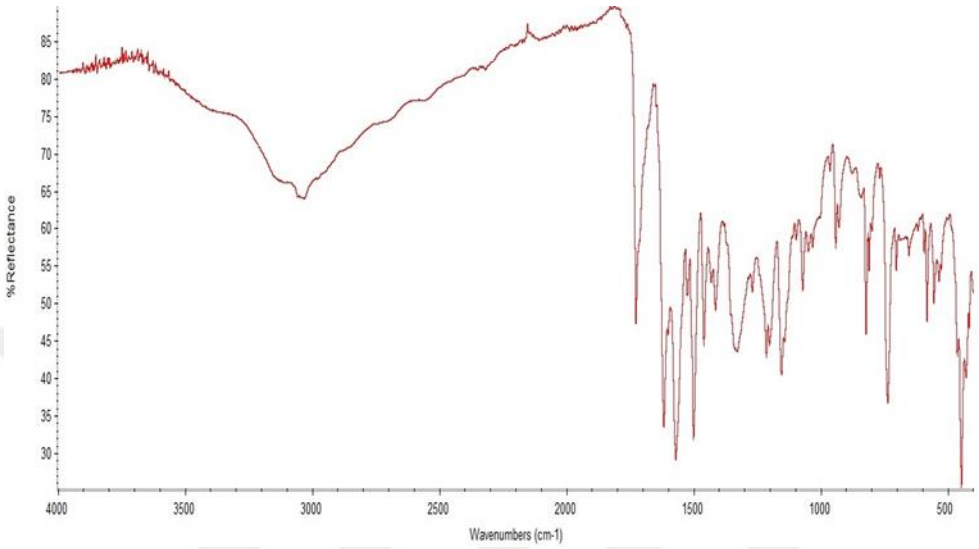

Attachment 12. FT-IR spectrum of (E)-8-(((3-bromophenyl)imino)methyl)-7-hydroxy-4-methyl-2H-chromen-2-one (3b)

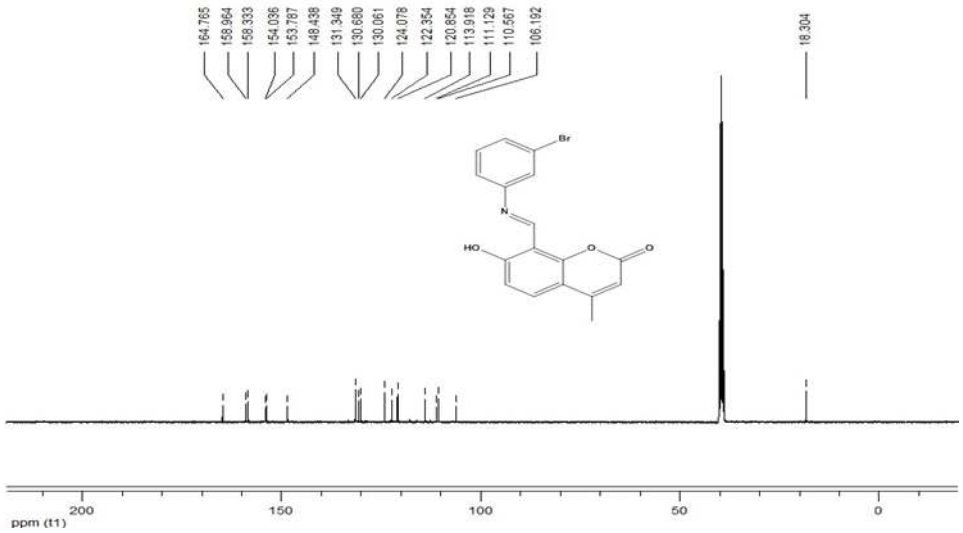

Attachment 13. ^{1}H NMR spectrum of (E)-8-(((3-chlorophenyl)imino)methyl)-7-hydroxy-4-methyl-2H-chromen-2-one (3c)

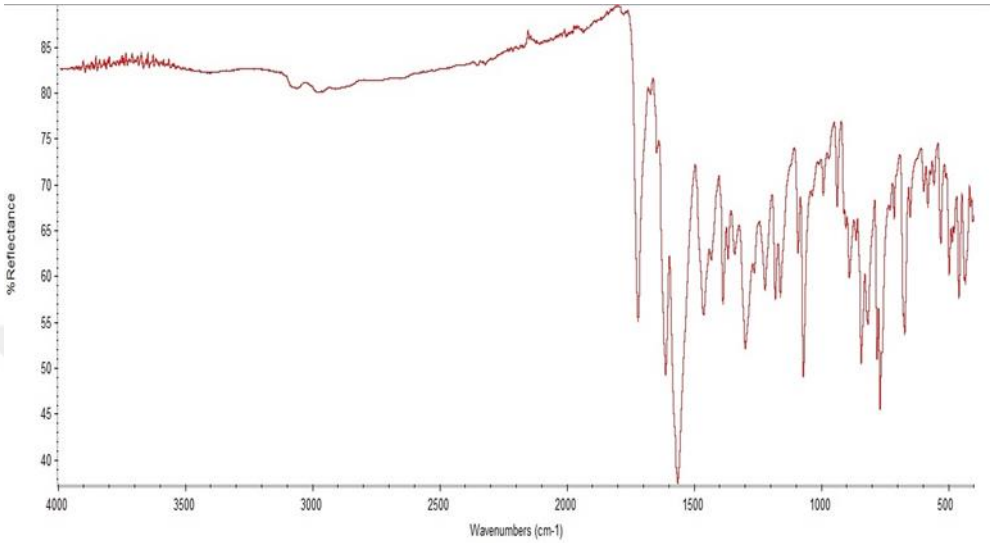

Attachment 14. ^{13}C NMR spectrum of (E)-8-(((3-chlorophenyl)imino)methyl)-7-hydroxy-4-methyl-2H-chromen-2-one (3c)

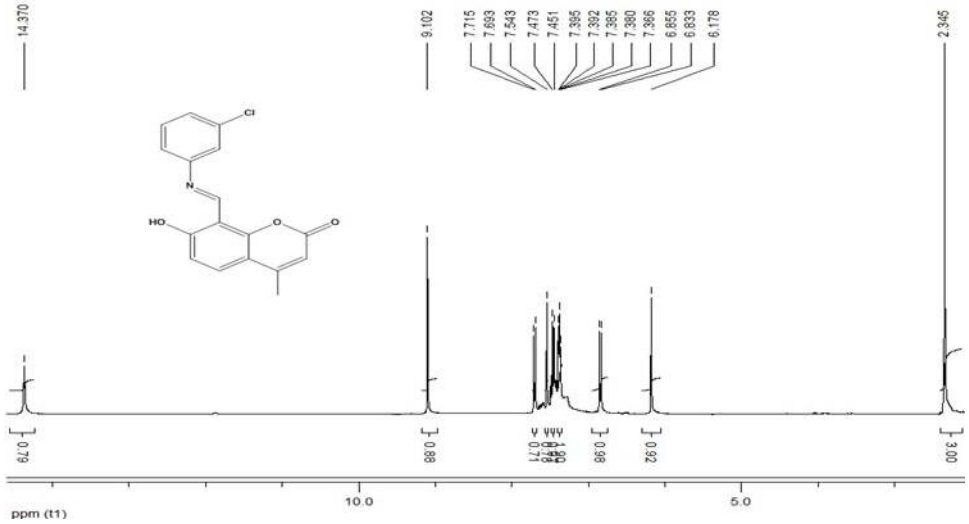

Attachment 15. FT-IR spectrum of (E)-8-(((3-chlorophenyl)imino)methyl)-7-hydroxy-4-methyl-2H-chromen-2-one (3c)

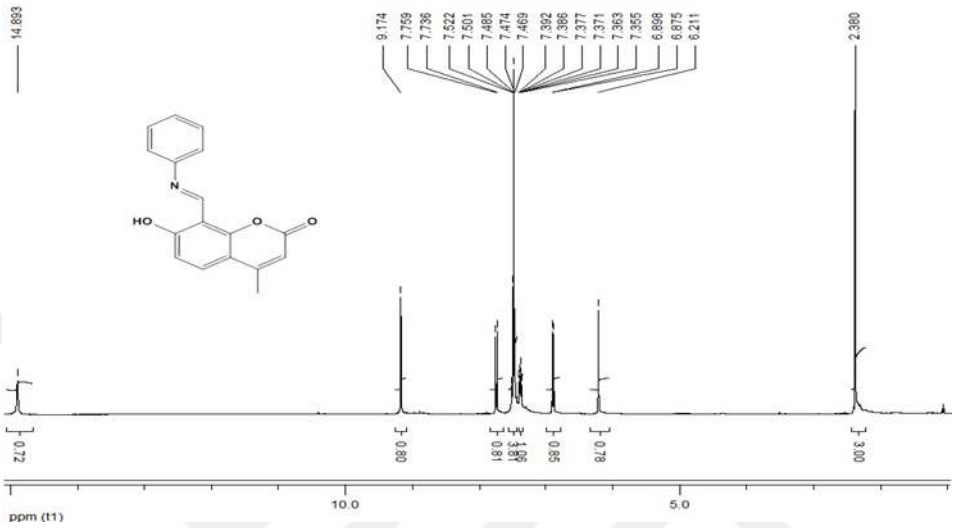

Attachment 16. ^{1}H NMR spectrum of (E)-7-hydroxy-4-methyl-8-((phenylimino)methyl)-2H-chromen-2-one (3d)

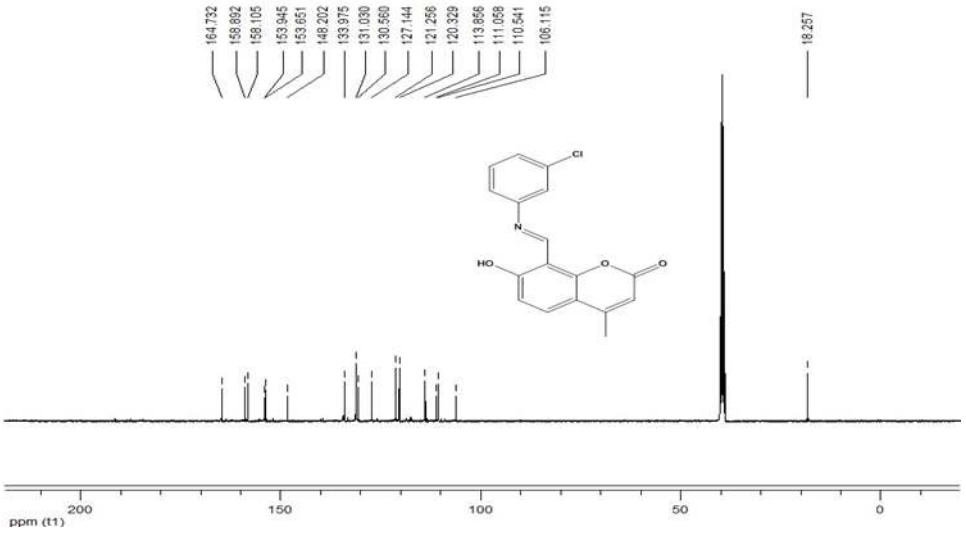

Attachment 17. ^{13}C NMR spectrum of (E)-7-hydroxy-4-methyl-8-((phenylimino)methyl)-2H-chromen-2-one (3d)

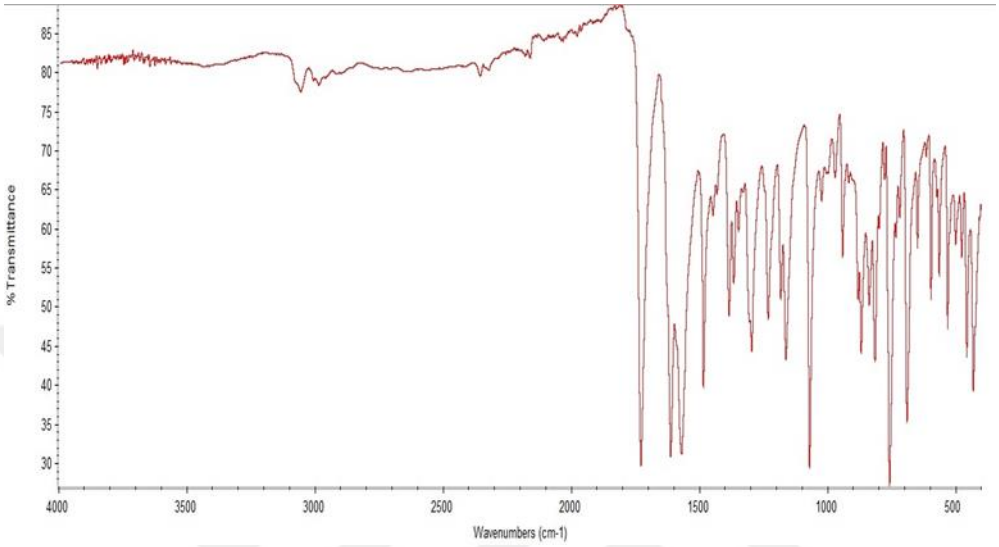

Attachment 18. FT-IR spectrum of (E)-7-hydroxy-4-methyl-8-((phenylimino)methyl)-2H-chromen-2-one (3d)

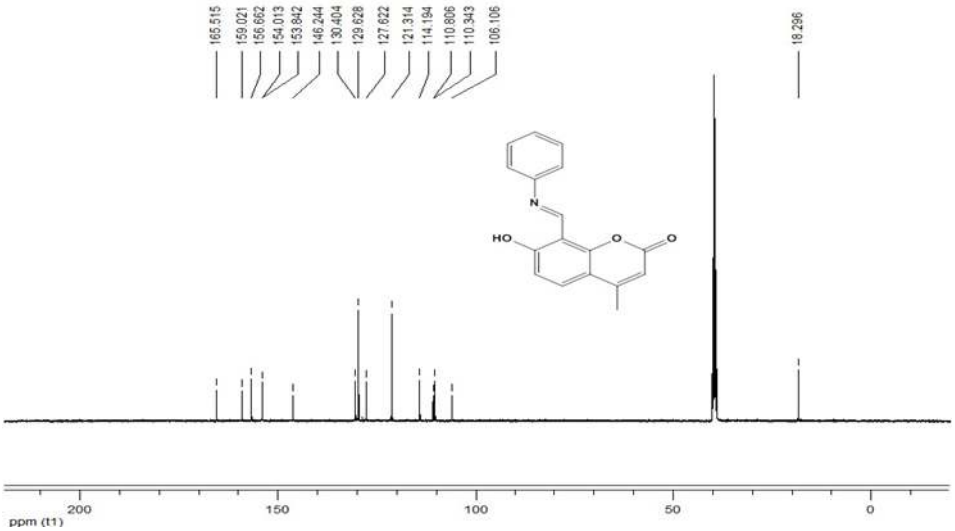

Attachment 19. ^{1}H NMR spectrum of (E)-7-hydroxy-4-methyl-8-(((3-methylpyridin-2-yl)imino)methyl)-2H-chromen-2-one (3e)

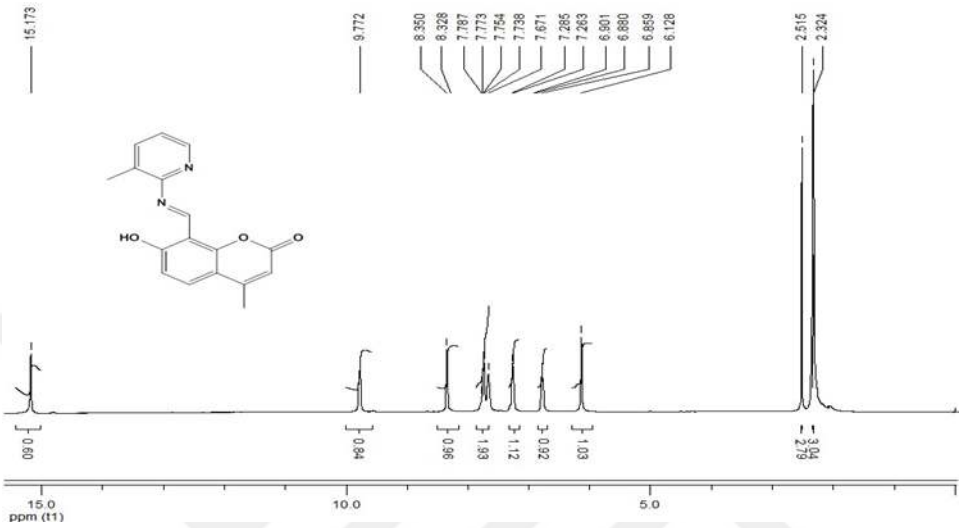

Attachment 20. ^{13}C NMR spectrum of (E)-7-hydroxy-4-methyl-8-(((3-methylpyridin-2-yl)imino)methyl)-2H-chromen-2-one (3e)

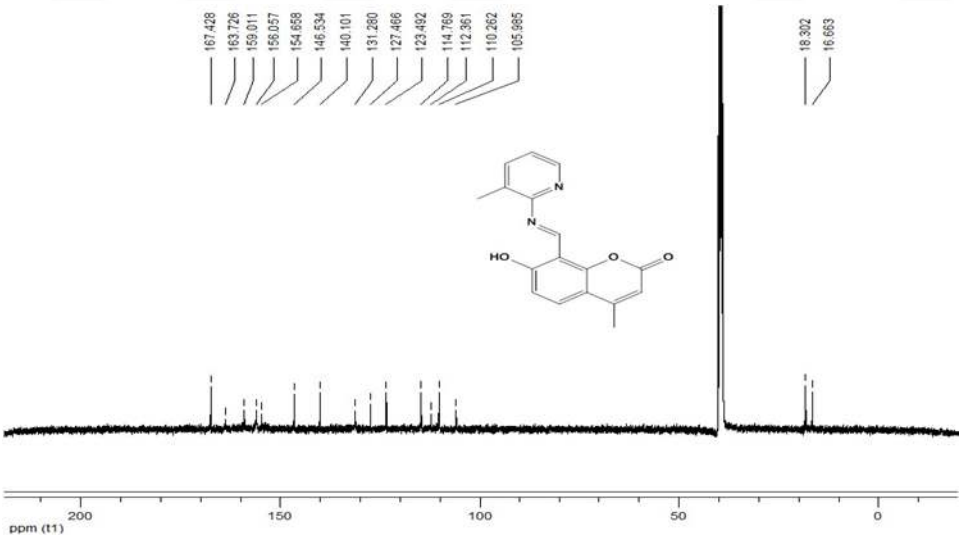

Attachment 21. FT-IR spectrum of (E)-7-hydroxy-4-methyl-8-(((3-methylpyridin-2-yl)imino)methyl)-2H-chromen-2-one (3e)

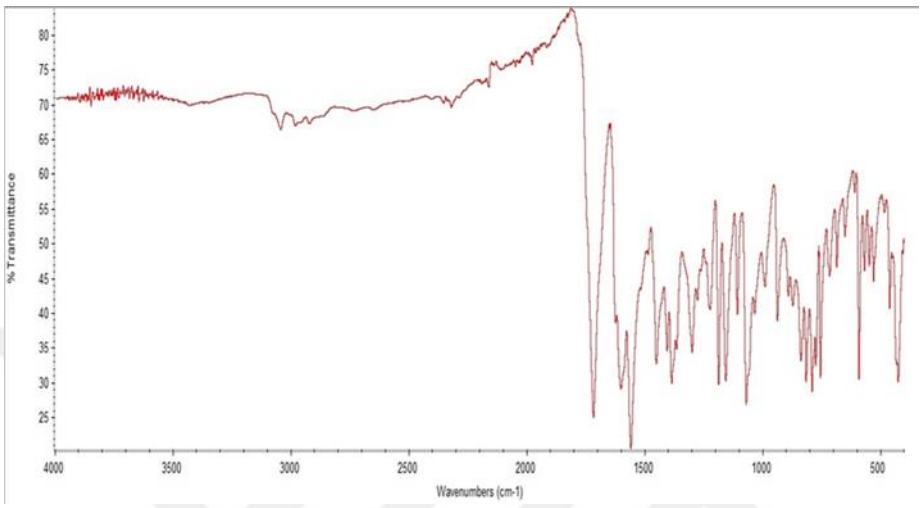

Attachment 22. ^{1}H NMR spectrum of (E)-8-((2-(2,4-dinitrophenyl) hydrazono)methyl)-7-hydroxy-4-methyl-2H-chromen-2-one (4a)

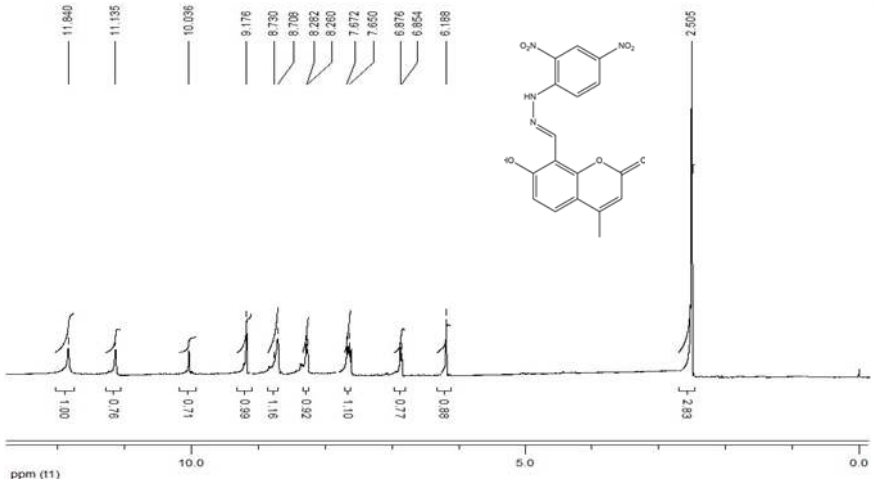

Attachment 23. ^{13}C NMR spectrum of (E)-8-((2-(2,4-dinitrophenyl) hydrazono)methyl)-7-hydroxy-4-methyl-2H-chromen-2-one (4a))

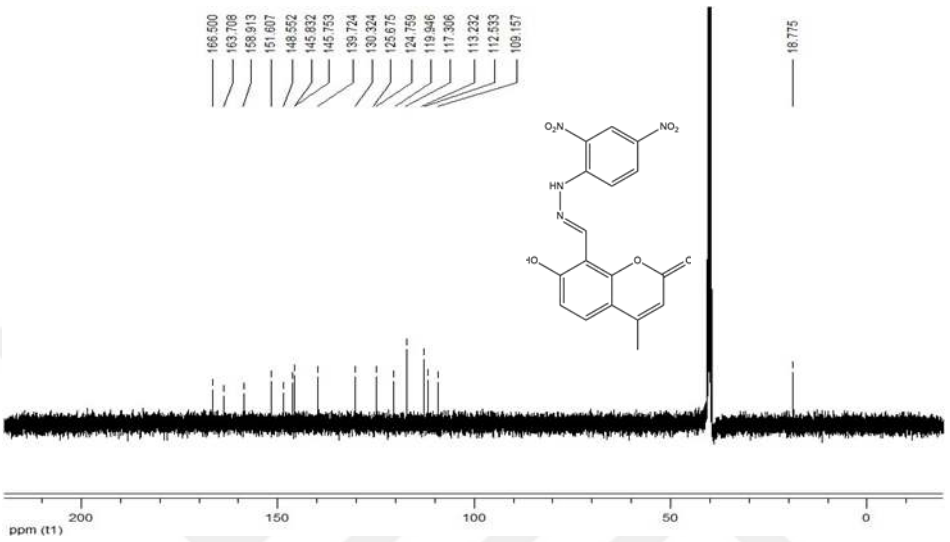

Attachment 24. FT-IR spectrum of (E)-8-((2-(2,4-dinitrophenyl)hydrazono) methyl)-7-hydroxy-4-methyl-2H-chromen-2-one (4a)

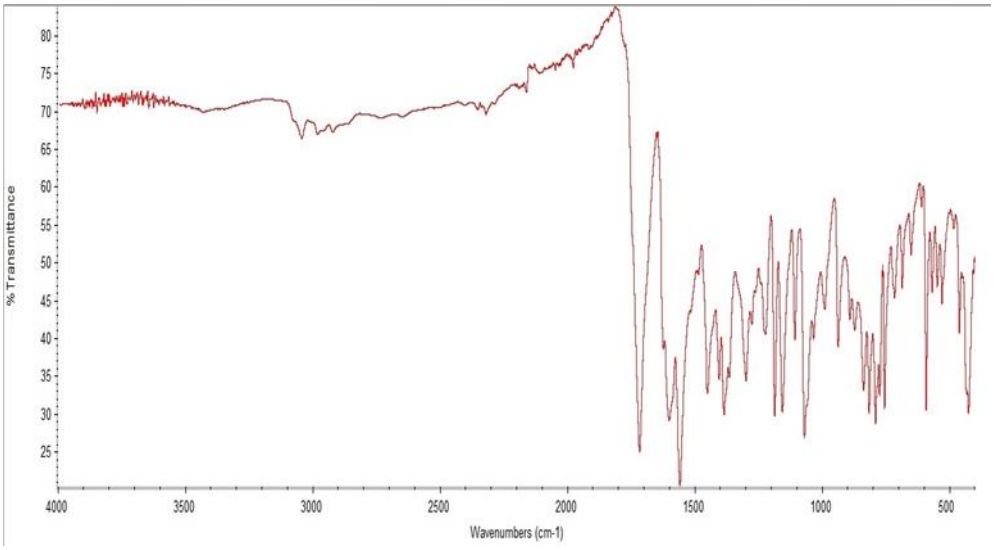

Attachment 25. ^{1}H NMR spectrum of (E)-7-hydroxy-4-methyl-8-((2-phenylhydrazono) methyl)-2H-chromen-2-one (4b)

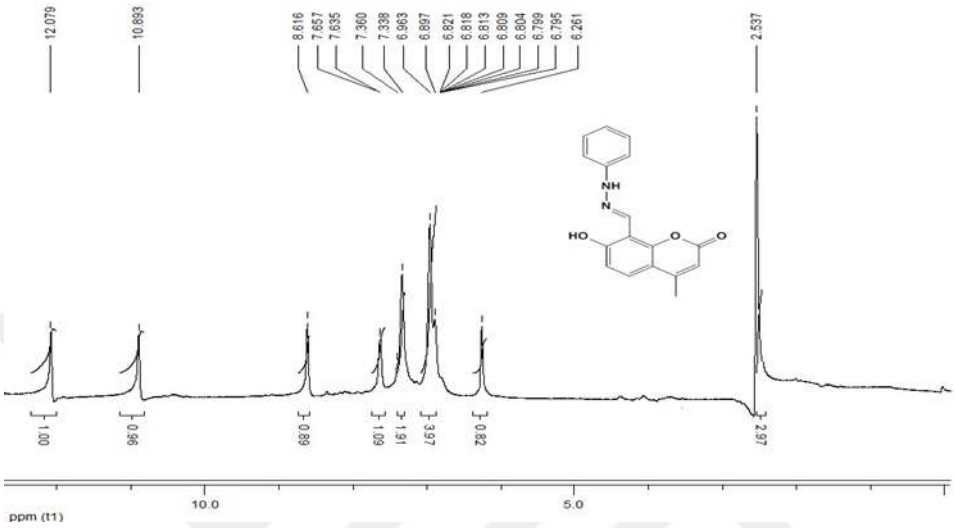

Attachment 26. ^{13}C NMR spectrum of (E)-7-hydroxy-4-methyl-8-((2-phenylhydrazono) methyl)-2H-chromen-2-one (4b)

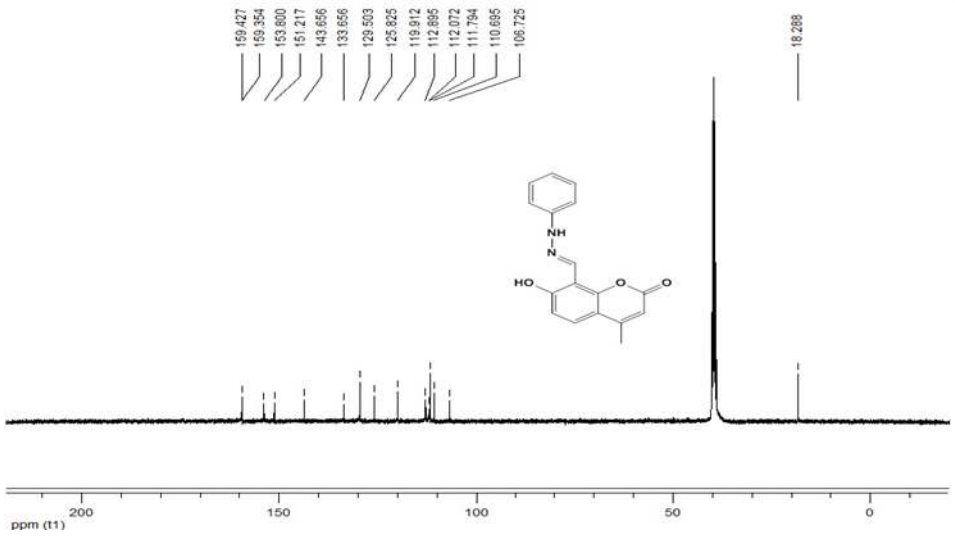

Attachment 27. FT-IR spectrum of (E)-7-hydroxy-4-methyl-8-((2-phenylhydrazono) methyl)-2H-chromen-2-one (4b)

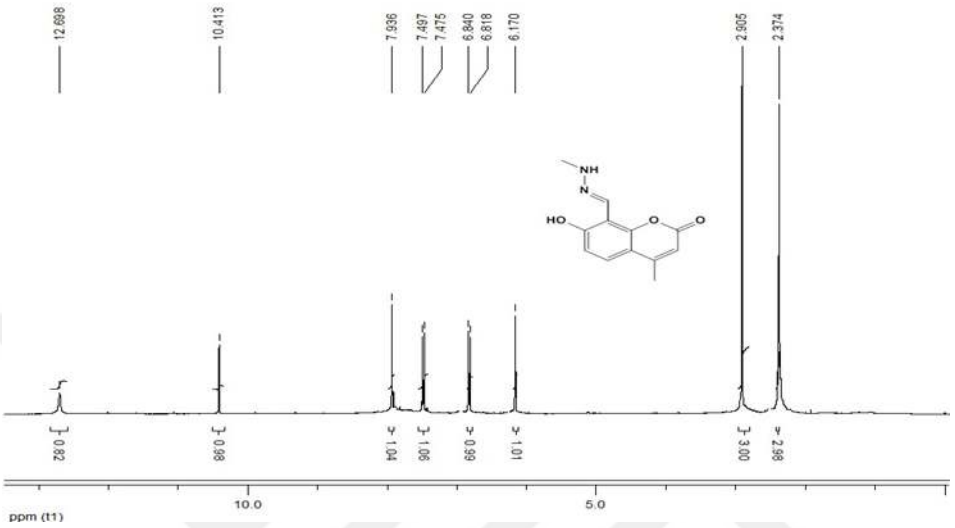

Attachment 28. ^{1}H NMR spectrum of (E)-7-hydroxy-4-methyl-8-((2-methylhydrazono) methyl)-2H-chromen-2-one (4c)

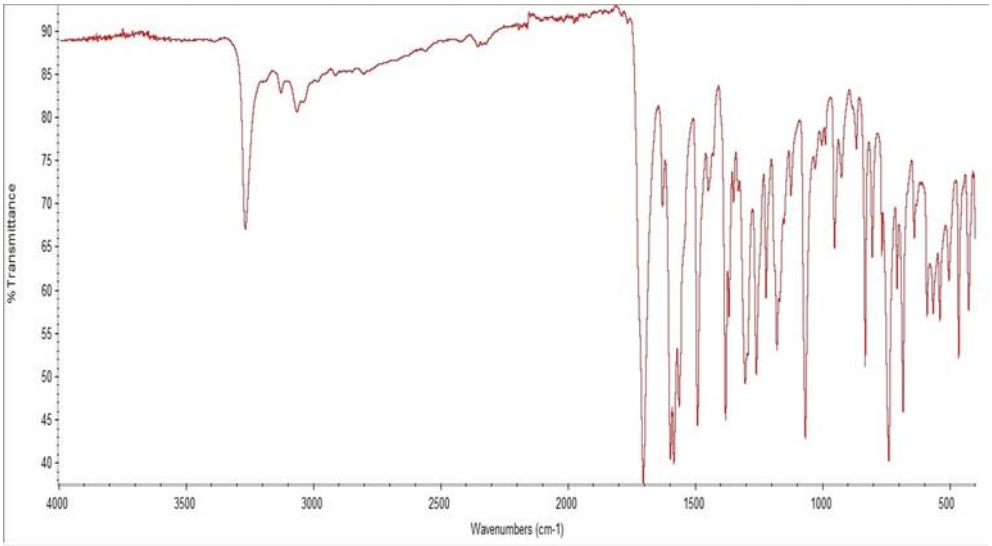

Attachment 29. ^{13}C NMR spectrum of (E)-7-hydroxy-4-methyl-8-((2-methylhydrazono) methyl)-2H-chromen-2-one (4c)

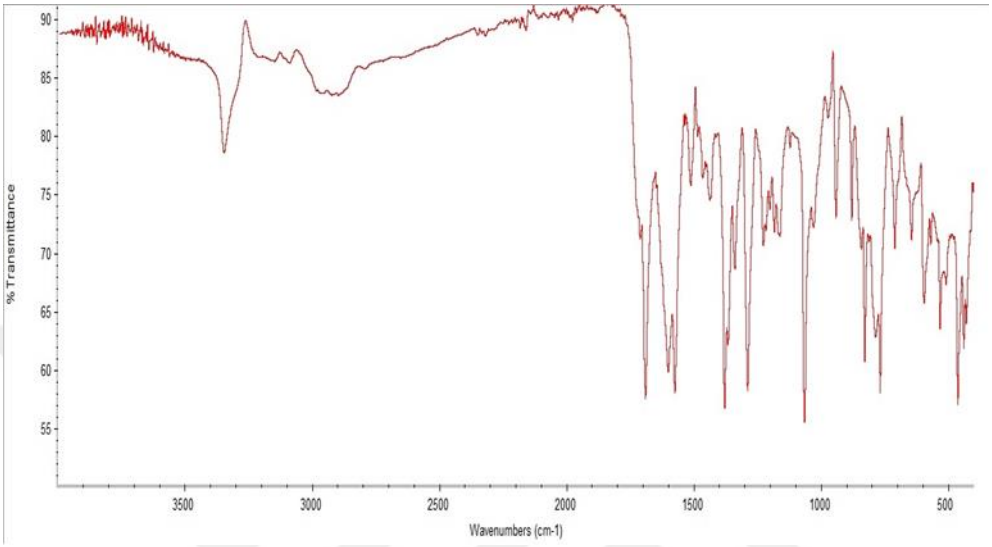

Attachment 30. FT-IR spectrum of (E)-7-hydroxy-4-methyl-8-((2-methylhydrazono) methyl)-2H-chromen-2-one (4c)

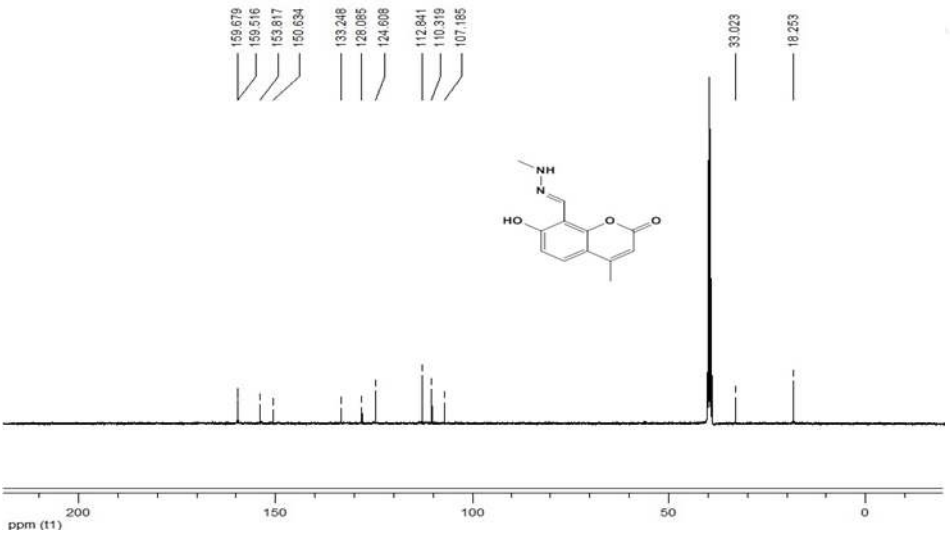

Attachment 31. ^{1}H NMR spectrum of (E)-7-hydroxy-4-methyl-8-((2-(pyridin-2-yl)hydrazono) methyl)-2H-chromen-2-one (4d)

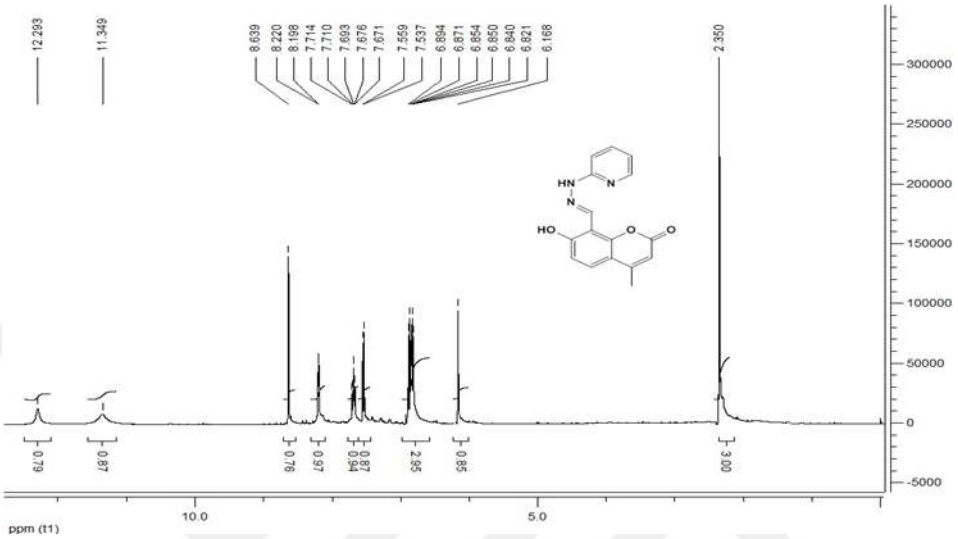

Attachment 32. ^{13}C NMR spectrum of (E)-7-hydroxy-4-methyl-8-((2-(pyridin-2-yl)hydrazono) methyl)-2H-chromen-2-one (4d)

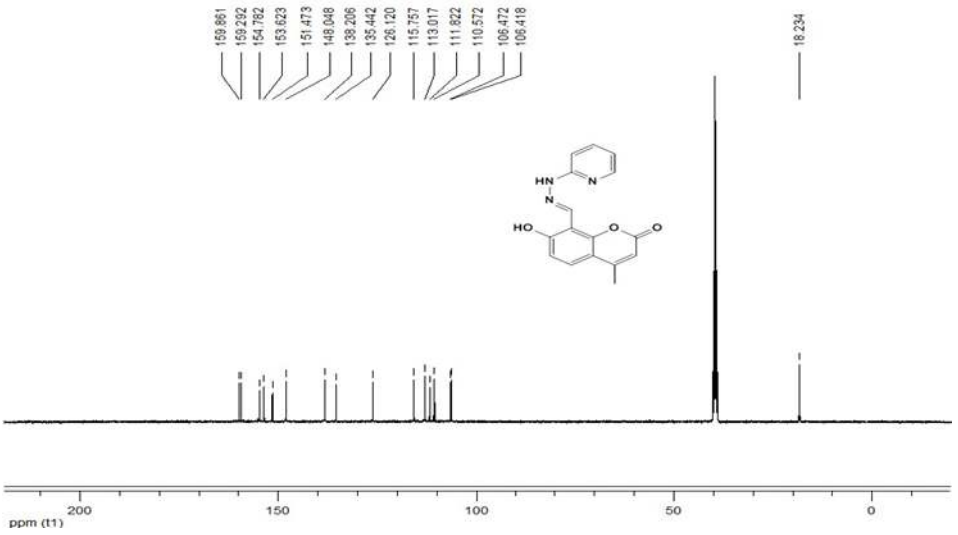

Attachment 33. FT-IR spectrum of (E)-7-hydroxy-4-methyl-8-((2-(pyridin-2-yl)hydrazono) methyl)-2H-chromen-2-one (4d)

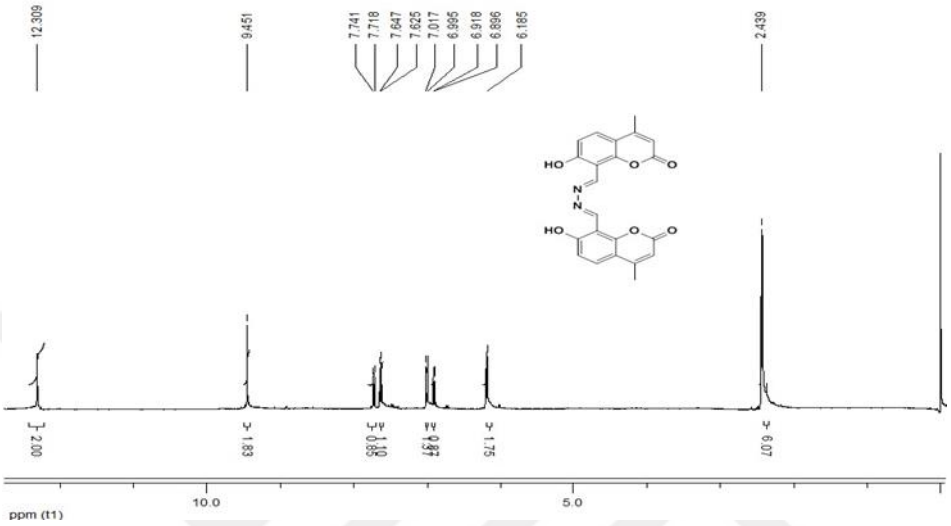

Attachment 34. ^{1}H NMR spectrum of 8,8'-((1E,1'E)-hydrazine-1,2-diylidenebis (methanylylidene))bis(7-hydroxy-4-methyl-2H-chromen-2-one) (4e)

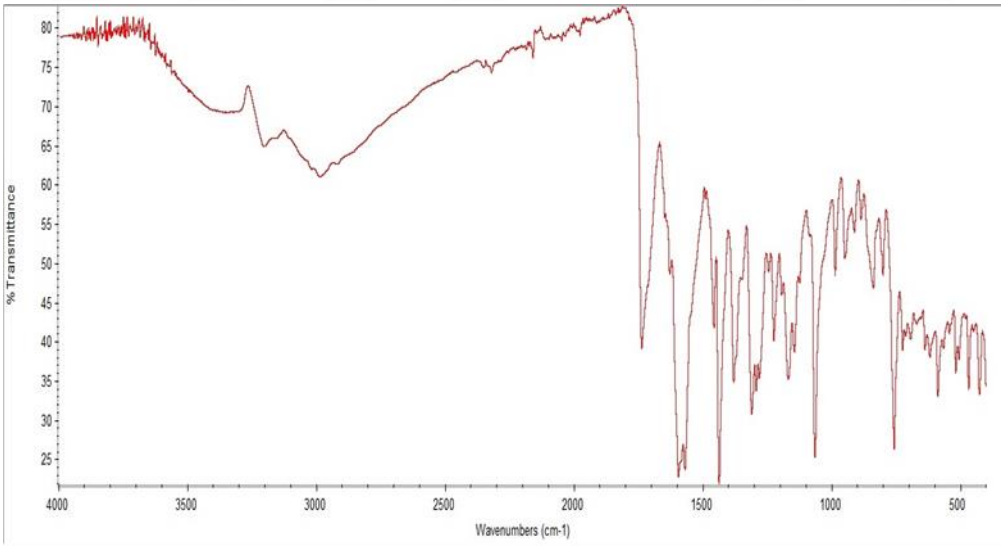

Attachment 35. ^{13}C NMR spectrum of 8,8'-((1E,1'E)-hydrazine-1,2-diylidenebis (methanylylidene))bis(7-hydroxy-4-methyl-2H-chromen-2-one) (4e)

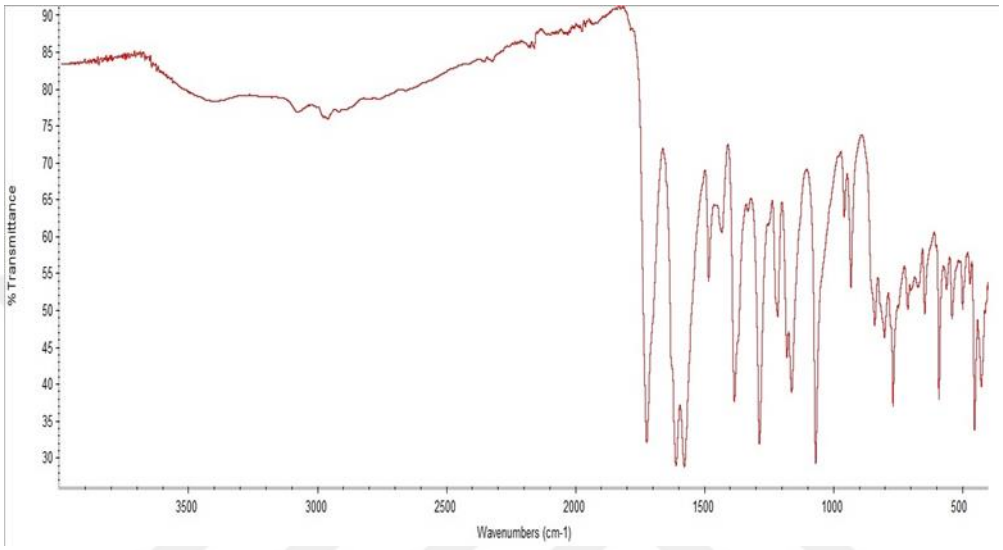

Attachment 36. FT-IR spectrum of 8,8'-((1E,1'E)-hydrazine-1,2-diylidenebis (methanylylidene))bis(7-hydroxy-4-methyl-2H-chromen-2-one) (4e)